

Anomalous extinction behaviour towards the Type Ia SN 2003cg.

N. Elias-Rosa^{1,2}, S. Benetti¹, E. Cappellaro¹, M. Turatto¹, P. A. Mazzali^{3,4},
F. Patat⁵, W.P.S. Meikle⁶, M. Stehle³, A. Pastorello³, G. Pignata⁷,
R. Kotak⁵, A. Harutyunyan¹, G. Altavilla⁸, H. Navasardyan¹, Y. Qiu⁹,
M. E. Salvo¹⁰ and W. Hillebrandt³.

¹INAF - Osservatorio Astronomico di Padova, vicolo dell'Osservatorio 5, I-35122 Padova, Italy

²Universidad de La Laguna, Av Astrofísico Francisco Sánchez s/n, E-38206. La Laguna, Tenerife, Spain

³Max-Planck-Institut für Astrophysik, Karl-Schwarzschild-Str. 1, D-85748 Garching bei München, Germany

⁴INAF - Osservatorio Astronomico di Trieste, via Tiepolo 11, I-34131 Trieste, Italy

⁵European Southern Observatory, Karl-Schwarzschild-Str. 2, D-85748 Garching bei München, Germany

⁶Astrophysics Group, Imperial College London, Blackett Laboratory, Prince Consort Road, London, SW7 2AZ, U.K.

⁷Departamento de Astronomía y Astrofísica, Pontificia Universidad Católica, Chile

⁸Departament d'Astronomia i Meteorologia, Universitat de Barcelona, Martí i Franquès 1, E-08028 Barcelona, Spain

⁹National Astronomical Observatories, Chinese Academy of Sciences, 100012 Beijing, China

¹⁰Australian National University, Mount Stromlo Observatory, Cotter Road, Weston ACT 2611 Canberra, Australia

Received; accepted

ABSTRACT

We present optical and near-infrared photometry and spectroscopy of the Type Ia SN 2003cg, which exploded in the nearby galaxy NGC 3169. The observations cover a period between -8.5 and +414 days post-maximum. SN 2003cg is a normal but highly-reddened Type Ia event. Its B magnitude at maximum $B_{max}=15.94\pm0.04$ and $\Delta m_{15}(B)_{obs} = 1.12\pm0.04$ ($\Delta m_{15}(B)_{intrinsic} = 1.25\pm0.05$). Allowing R_V to become a free parameter within the Cardelli et al. (1989) extinction law, simultaneous matches to a range of colour curves of normal SNe Ia yielded $E(B-V)=1.33\pm0.11$, and $R_V=1.80\pm0.19$. While the value obtained for R_V is small, such values have been invoked in the past, and may imply a grain size which is small compared with the average value for the local ISM.

Key words: supernovae: general – supernovae: individual: SN 2003cg – extinction

1 INTRODUCTION

Type Ia Supernovae (hereafter SNeIa) became very popular in the last decade because of their role in determining the geometry of the Universe. Because of their high luminosity and relatively small dispersion at maximum, SNeIa are the most accurate cosmological distance indicators currently available. Systematic studies of these events at high redshifts ($z \sim 0.3 - 1.6$), together with cosmic microwave background data and cluster masses and abundances, have provided strengthening evidence that the expansion of the Universe began to accelerate at half its present age. This finding is commonly related to a positive cosmological constant Λ (Riess et al. 1998; Perlmutter et al. 1999) and is generally attributed to a new form of dark energy (Knop et al. 2003).

in the cosmological use of SNe Ia: 1) that the properties of high- z SNe Ia are the same as those of their present-time counterparts is, to some extent, an assumption. Observational confirmation is highly desirable; 2) the use of SNe Ia as cosmological distance indicators relies on an empirical relation between the luminosity and the light curve shape which is only partly understood; 3) the progenitor systems of SNe Ia have not yet been unambiguously identified, nor have and the explosion mechanisms been clearly determined; 4) the extent to which observations of SNe Ia are affected by dust extinction is still unresolved.

The theoretical and observational investigation of local SNe Ia is the main motivation of the European Supernova Collaboration (ESC)¹. This collaboration was born under the conviction that the only way to make a

decisive jump in understanding the physics of SNe Ia is to compare realistic models of thermonuclear explosions (and the emerging radiation) with a complete and detailed set of homogeneously-acquired observations. The first two years of the ESC produced excellent results, with fourteen well-monitored targets, e.g. Benetti et al. (2004), Pignata et al. (2004a) and Kotak et al. (2005).

In this paper, we present optical and infrared photometry and spectroscopy of SN 2003cg, the fourth supernova monitored by the ESC. It is exceptional in that it is heavily reddened.

2 OBSERVATIONS

SN 2003cg was discovered on 2003 March 21.51 UT by Itagati and Arbour (IAUC 8097) at 14" E and 5" N from the centre of the nearby spiral galaxy NGC 3169 (Figure 1). The SN is projected on a dust lane, already suggesting that the SN light might be heavily extinguished. Some days later, Kotak, Meikle & Patat (2003) and Matheson et al. (2003) classified SN 2003cg as a highly-reddened 'normal' Type Ia SN, of epoch a few days before maximum.

NGC 3169 is a nearby ($v_r=1238 \text{ km s}^{-1}$), elongated Sa galaxy with narrow, distorted arms. It has a total B magnitude of 11.08 with a prominent dust lane. SN 1984E also exploded in NGC 3169. This was a Type IIL SN with a B magnitude at maximum of 15.2. Comparison of the intrinsic colour curve with those of other Type II SNe (Metlova 1985) yielded $E(B-V)=0.1\pm0.05$ for this older event. It exhibited evidence of pre-explosion superwinds (Dopita et al. 1984; Gaskell 1984; Gaskell & Keel 1986; Henry & Branch 1987) similar to those of SNe 1994aj, 1996L and 1996al (Benetti 2000).

In view of the favorable SN position on the sky ($\alpha = 10^h 14^m 15^s.97$, $\delta = +03^\circ 28' 02''.50$, 2000.0), the early discovery epoch and the proximity of the host galaxy ($v_r=1238 \text{ km s}^{-1}$), an extensive observational campaign was immediately triggered with all the telescopes available to the ESC. Using 13 different instrumental configurations, we obtained optical and NIR data from day -8.5 to +414 relative to B band maximum light. The observational programme comprised 74 photometric epochs and 35 spectra.

The SN 2003cg observations were processed using IRAF² and FIGARO³ routines. For photometry we used a collection of tasks developed in the IRAF environment by the Padova-Asiago SN Group.

2.1 Photometric observations

Standard pre-processing (trimming, overscan and bias corrections, flat-fielding) was first carried out. Then, for

the early-time optical photometry, the instrumental optical magnitudes of the SN and the local standards were measured using the IRAF point-spread-function (PSF) fitting routine. Specifically, after fitting and subtracting the background galaxy contamination, we used Daophot to fit the SN profile with a PSF obtained from a set of local, unsaturated stars. These local standards in the SN field (see Figure 1) were also used to calibrate the SN brightness on non-photometric nights. To calibrate the local standards, and to find the colour terms for the various instrumental setups, average values for 20 photometric nights were obtained (marked in Table 1). These were then calibrated via standard Landolt fields (Landolt 1992). Magnitudes and estimated errors for the local sequence stars are given in Table 2.

For the early-time IR magnitudes, additional reduction steps were required viz. sky subtraction, and image coaddition to improve the signal-to-noise (see Table 3). As for the optical photometry, the IR magnitudes were obtained using PSF-fitting. For night-to-night calibration we used a smaller local sequence. However, as the number of IR standard fields observed each night was small, we adopted average colour terms provided by the telescope teams. The IR magnitudes of the local sequence stars are given in Table 2.

SN 2003cg was also observed at late phases. In this case, determination of the SN magnitudes made use of template subtraction. The procedure makes use of the ISIS template subtraction program (Alard 2000) and runs in the IRAF environment. A reference image of the host galaxy is obtained long after the SN image. The two images are then registered geometrically and photometrically. The better-seeing image is degraded to that of the poorer one. Finally the reference (template) image is subtracted from the SN image. The template images were taken with VLT-UT2+FORIS on February 1, 2005, around 673 days post-explosion, when the supernova was no longer visible. The technique was first tested for early phase images when the SN was bright. It was found that the PSF-fitting and template-subtraction methods produced results in excellent agreement even with a variety of instrumental configurations. The late-time magnitudes of SN 2003cg are shown in Table 1.

Uncertainties in the instrumental photometry were estimated by placing artificial stars with the same magnitude and profile as the SN, at positions close (within a few arcsec) to that of the SN, and then computing the deviations of the artificial star magnitudes. For the calibration error we adopted the r.m.s. of the observed magnitudes of the local sequence stars obtained during photometric nights only.

2.2 Spectroscopic observations

The spectra were reduced using standard IRAF (used for optical and IR reduction) or FIGARO (used for IR reduction only) routines. This includes bias, overscan (only for the optical spectra) and flat field correction. We then fitted a polynomial function to the background

² IRAF is distributed by the National Optical Astronomy Observatories, which are operated by the Association of Universities for Research in Astronomy, Inc, under contract with the National Science Foundation.

³ <http://www.aao.gov.au/figaro/>

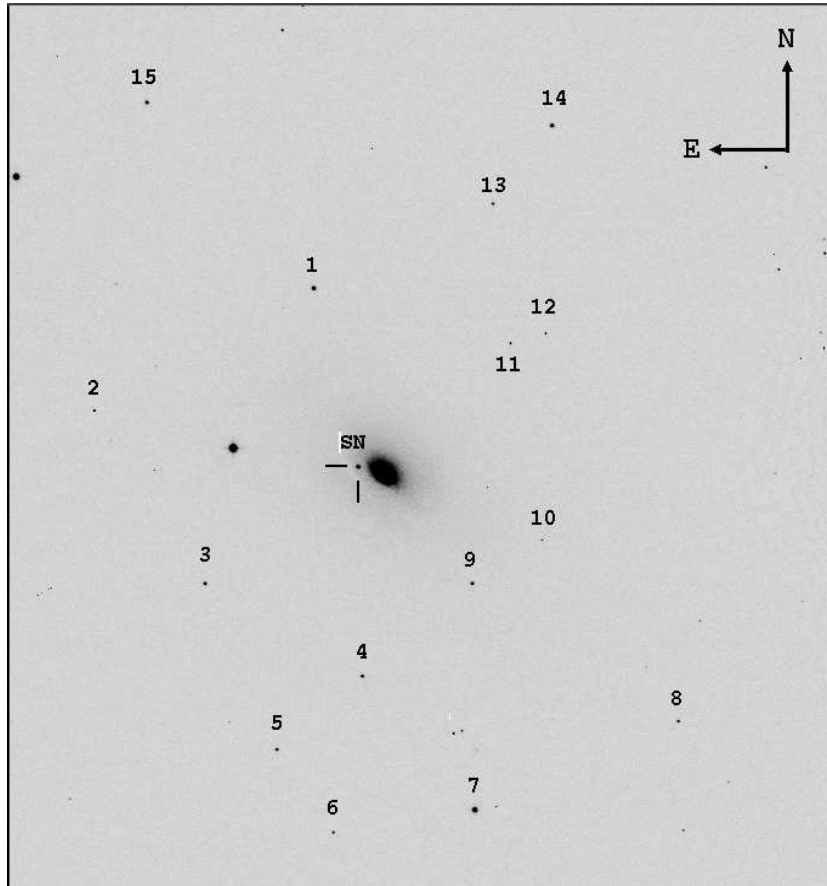


Figure 1. V band image of SN 2003cg in NGC 3169 taken with the ESO/MPI 2.2m+WFI on 2003 April 03 (FoV $\sim 8'.5 \times 9'.0$). Local sequence stars are indicated (cf. Table 2).

flux including that of the galaxy, and removed the interpolated background by subtraction. Extraction from the bi-dimensional spectra made use of an optimised extraction algorithm. The one-dimensional spectra were wavelength calibrated by comparison with arc-lamp spectra, and flux calibrated using spectrophotometric standard stars. For most spectra the errors in the wavelength calibration are $< \pm 2 \text{ \AA}$. The standard star spectra were also used to model and remove the telluric absorptions. The absolute flux calibration of the spectra was checked against photometry and when necessary, the flux scale was adjusted. After that, the calibration is typically accurate within $\pm 10\text{-}20\%$. The spectroscopic observations are summarised in Tables 4 & 5. The tables give the observation date, the Modified Julian Day, the phase relative to B_{max} , the wavelength range and the instruments used.

2.3 Correction to standard photometric bands

As indicated in Tables 1 & 3, we used ten different instruments to collect the photometry of SN 2003cg from U to K band. It is desirable to convert the photometry of the target to a standard system. However, this is made difficult by the non-stellar form of the SN Ia spectrum. Nevertheless, several authors have shown that, with care, such a correction can minimise systematic errors (Suntzeff 2000;

Stritzinger et al. 2002; Krisciunas et al. 2003; Pignata et al. 2004a; Pignata 2004b). The procedure involved is sometimes called the S-correction (Stritzinger et al. 2002). We applied S-corrections to our data following the method of Pignata et al. (2004a). The main challenge was to determine the instrument/filter/detector system efficiency for each observation. Once the instrumental response functions were constructed, we calculated an instrumental zero-point for each passband. We then derived synthetic colour terms for the optical using a set of spectrophotometric standard stars (Hamuy et al. 1992; Hamuy et al. 1994) and for the IR, using the spectra of Vega, Sirius and the Sun. With this information we then calculated the S-corrections for the BVRI-JHK bands⁴ by using the best flux-calibrated spectra of SN 2003cg. As the epochs of these spectra did not fully match the early-time photometric coverage, we enhanced the S-correction spectral database by adding a set of spectra of SN 1994D (Patat et al. 1996), artificially reddened to match those of SN 2003cg (see Section 3 for more details). The features of the SNe 1994D and 2003cg spectra are very similar. At late times (nebular era) we have only one optical spectrum of SN 2003cg. We therefore used the spectra of other normal SNe Ia: 1992A (Suntzeff 1996);

⁴ We did not compute an S-correction for the U band since very few spectra covered this wavelength range.

Table 1. Original optical photometry of SN 2003cg.

date	MJD	Phase* (days)	U	B	V	R	I	Instr.
13/03/03	52711.30	-18.1	-	-	-	19.0	-	UNF
22/03/03	52720.30	-9.1	-	-	-	14.9	-	UNF
23/03/03<	52721.94	-7.5	17.03 ± 0.19	16.49 ± 0.06	15.27 ± 0.04	14.58 ± 0.02	14.14 ± 0.07	CAF
24/03/03<	52722.54	-6.9	16.91 ± 0.08	16.35 ± 0.03	15.24 ± 0.03	14.55 ± 0.02	14.07 ± 0.02	SSO
24/03/03	52722.56	-6.9	-	16.34 ± 0.03	15.21 ± 0.04	14.50 ± 0.03	14.00 ± 0.03	BAO
25/03/03<	52723.44	-6.0	16.77 ± 0.04	16.22 ± 0.01	15.09 ± 0.01	14.44 ± 0.02	13.95 ± 0.01	SSO
26/03/03	52724.53	-4.9	-	16.13 ± 0.20	14.99 ± 0.36	14.29 ± 0.06	-	BAO
26/03/03	52724.82	-4.7	-	16.09 ± 0.02	14.92 ± 0.03	14.29 ± 0.02	13.85 ± 0.03	ASI
27/03/03	52725.85	-3.6	-	16.03 ± 0.02	14.84 ± 0.03	14.27 ± 0.02	13.84 ± 0.04	ASI
28/03/03<	52726.02	-3.5	16.67 ± 0.02	16.08 ± 0.03	14.85 ± 0.02	14.24 ± 0.03	13.77 ± 0.02	WFI
28/03/03	52726.51	-3.0	-	16.02 ± 0.19	14.82 ± 0.03	14.19 ± 0.04	13.82 ± 0.03	BAO
29/03/03	52727.02	-2.5	-	15.99 ± 0.04	14.78 ± 0.06	14.18 ± 0.03	13.84 ± 0.03	ASI
29/03/03	52727.57	-1.9	-	15.98 ± 0.06	14.82 ± 0.02	14.17 ± 0.05	13.80 ± 0.05	BAO
01/04/03	52730.83	1.4	-	15.97 ± 0.03	14.72 ± 0.05	14.15 ± 0.05	13.86 ± 0.03	ASI
02/04/03<	52731.16	1.7	16.79 ± 0.03	16.05 ± 0.02	14.74 ± 0.06	14.15 ± 0.02	13.88 ± 0.03	WFI
04/04/03<	52733.12	3.7	16.87 ± 0.09	16.10 ± 0.02	14.76 ± 0.03	14.18 ± 0.02	13.95 ± 0.04	WFI
04/04/03	52733.62	4.2	-	16.04 ± 0.05	14.79 ± 0.05	14.19 ± 0.04	13.97 ± 0.03	BAO
04/04/03	52733.89	4.4	16.89 ± 0.10	16.05 ± 0.03	14.83 ± 0.03	14.24 ± 0.03	14.00 ± 0.06	TGD
07/04/03	52736.51	7.1	-	16.22 ± 0.08	14.93 ± 0.04	14.35 ± 0.05	14.12 ± 0.03	BAO
07/04/03	52736.80	7.3	-	16.25 ± 0.04	14.92 ± 0.04	14.39 ± 0.07	14.08 ± 0.05	ASI
09/04/03<	52738.90	9.4	17.26 ± 0.02	16.45 ± 0.01	14.99 ± 0.03	14.56 ± 0.02	14.27 ± 0.04	TGD
11/04/03	52740.87	11.4	17.51 ± 0.01	16.65 ± 0.05	15.13 ± 0.03	14.68 ± 0.04	14.37 ± 0.03	TGD
12/04/03<	52741.90	12.4	17.69 ± 0.04	16.79 ± 0.01	15.17 ± 0.02	14.73 ± 0.04	14.33 ± 0.06	CAF
14/04/03<	52743.07	13.6	18.06 ± 0.13	16.93 ± 0.01	15.19 ± 0.02	14.78 ± 0.01	14.36 ± 0.02	WFI
15/04/03	52744.02	14.6	18.10 ± 0.03	17.13 ± 0.01	15.26 ± 0.02	14.81 ± 0.01	14.37 ± 0.02	WFI
16/04/03	52745.08	15.6	18.40 ± 0.03	17.22 ± 0.04	15.30 ± 0.03	14.82 ± 0.02	14.30 ± 0.03	WFI
17/04/03	52746.09	16.6	18.78 ± 0.05	17.34 ± 0.03	15.33 ± 0.02	14.83 ± 0.02	14.24 ± 0.02	WFI
18/04/03	52747.11	17.6	18.93 ± 0.04	17.42 ± 0.02	15.41 ± 0.02	14.84 ± 0.01	14.24 ± 0.02	WFI
19/04/03	52748.04	18.6	19.04 ± 0.02	17.57 ± 0.02	15.42 ± 0.03	14.85 ± 0.02	14.22 ± 0.02	WFI
20/04/03<	52749.07	19.6	19.26 ± 0.05	17.68 ± 0.03	15.47 ± 0.01	14.85 ± 0.01	14.20 ± 0.02	WFI
21/04/03<	52750.14	20.7	19.29 ± 0.02	17.77 ± 0.02	15.53 ± 0.02	14.87 ± 0.02	14.17 ± 0.01	WFI
21/04/03	52750.98	21.5	19.30 ± 0.03	17.92 ± 0.02	15.54 ± 0.02	14.90 ± 0.02	14.17 ± 0.01	WFI
23/04/03<	52752.01	22.5	19.48 ± 0.02	17.98 ± 0.01	15.60 ± 0.01	14.90 ± 0.01	14.15 ± 0.01	WFI
23/04/03	52752.95	23.5	-	18.09 ± 0.08	-	14.93 ± 0.02	14.16 ± 0.03	ASI
24/04/03<	52753.19	23.7	19.57 ± 0.09	18.17 ± 0.02	15.65 ± 0.03	14.92 ± 0.01	14.11 ± 0.02	WFI
25/04/03<	52754.01	24.5	19.73 ± 0.03	18.26 ± 0.01	15.69 ± 0.08	14.93 ± 0.01	14.15 ± 0.01	WFI
25/04/03<	52755.00	25.5	19.84 ± 0.02	18.34 ± 0.01	15.78 ± 0.01	14.99 ± 0.02	14.13 ± 0.01	WFI
26/04/03	52755.85	26.4	-	-	15.90 ± 0.02	15.02 ± 0.02	-	CAF
27/04/03<	52756.11	26.6	19.91 ± 0.02	18.46 ± 0.01	15.82 ± 0.01	15.06 ± 0.01	14.12 ± 0.01	WFI
28/04/03<	52757.00	27.5	19.90 ± 0.02	18.57 ± 0.01	15.94 ± 0.01	15.09 ± 0.01	14.16 ± 0.01	WFI
29/04/03	52758.51	29.1	-	-	-	15.18 ± 0.03	14.23 ± 0.04	BAO
30/04/03	52759.13	29.7	20.24 ± 0.04	18.80 ± 0.01	16.08 ± 0.01	15.23 ± 0.01	14.25 ± 0.02	WFI
30/04/03	52759.50	30.0	-	-	16.12 ± 0.11	15.23 ± 0.04	14.30 ± 0.09	BAO
02/05/03	52761.15	31.7	20.28 ± 0.02	18.94 ± 0.03	16.14 ± 0.05	15.38 ± 0.02	14.44 ± 0.02	WFI
02/05/03	52761.99	32.5	20.31 ± 0.03	18.98 ± 0.05	16.19 ± 0.02	15.44 ± 0.02	14.52 ± 0.02	WFI
04/05/03	52763.01	33.5	20.48 ± 0.05	19.06 ± 0.03	16.25 ± 0.02	15.52 ± 0.02	14.58 ± 0.01	WFI
05/05/03	52764.99	35.5	20.43 ± 0.03	19.05 ± 0.02	16.41 ± 0.01	15.63 ± 0.03	14.70 ± 0.01	WFI
07/05/03<	52766.01	36.5	20.43 ± 0.03	19.04 ± 0.01	16.44 ± 0.01	15.69 ± 0.02	14.80 ± 0.01	WFI
07/05/03	52766.85	37.4	-	-	16.47 ± 0.07	-	-	ASI
07/05/03	52766.99	37.5	20.55 ± 0.05	19.10 ± 0.02	16.50 ± 0.01	15.73 ± 0.02	14.87 ± 0.02	WFI
08/05/03<	52767.85	38.4	-	19.10 ± 0.09	-	15.79 ± 0.03	14.91 ± 0.05	ASI
09/05/03	52768.37	38.9	-	19.05 ± 0.07	16.66 ± 0.03	15.80 ± 0.05	14.96 ± 0.01	SSO
17/05/03	52776.52	47.1	-	-	16.99 ± 0.04	16.15 ± 0.03	15.29 ± 0.05	BAO
22/05/03	52781.94	52.5	20.64 ± 0.07	19.26 ± 0.03	17.03 ± 0.04	16.37 ± 0.04	15.66 ± 0.04	TGD
23/05/03	52782.84	53.4	-	-	17.03 ± 0.10	16.39 ± 0.05	15.69 ± 0.03	ASI
31/05/03	52790.92	61.5	20.78 ± 0.09	19.33 ± 0.02	17.39 ± 0.04	16.60 ± 0.02	16.14 ± 0.08	TGO
07/06/03	52797.36	67.9	-	-	-	-	16.22 ± 0.12	SSO
19/06/03<	52809.02	79.6	-	19.58 ± 0.03	17.75 ± 0.01	17.21 ± 0.01	16.76 ± 0.02	WFI
25/06/03	52815.01	85.5	-	19.60 ± 0.02	17.95 ± 0.02	17.38 ± 0.03	16.91 ± 0.07	WFI

Table 1 – *continued*

date	MJD	Phase* (days)	U	B	V	R	I	Instr.
20/11/03	52963.20	233.7	-	-	21.09 ± 0.09	20.75 ± 0.06	-	ASI
31/01/04	53035.23	305.8	-	23.02 ± 0.18	21.68 ± 0.04	21.23 ± 0.28	20.01 ± 0.17	TGD
19/04/04	53114.08	384.6	-	24.12 ± 0.07	22.95 ± 0.12	22.59 ± 0.08	21.58 ± 0.02	FOR
07/05/04	53132.97	413.5	-	24.74 ± 0.17	22.92 ± 0.14	22.22 ± 0.05	21.89 ± 0.04	FOR
14/12/04	53353.29	623.8	-	> 23.60	> 22.63	> 23.18	> 21.53	WFI

* Relative to B_{max} (MJD=52729.40)

◁ Photometric night

UNF = Unfiltered CCD frames taken with a 0.60-m, Japan ((Itagati & Arbour 2003); CAF = Calar Alto 2.2m + CAFOS + CCD SITE 0.53''/px; SSO = Siding Spring Observatory 2.3m + CCD 0.59''/px; BAO = Beijing Astronomical Observatory 0.85m + CCD 0.45''/px; ASI = Asiago 1.82m Copernico telescope + AFOSC 0.47''/px; TGD = Telescopio Nazionale Galileo + DOLORES 0.28''/px; TGO = Telescopio Nazionale Galileo + OIG 0.07''/px; WFI = ESO/MPI 2.2m + WFI 0.24''/px; FOR = ESO VLT-UT2 + FORS1 0.20''/px

Table 2. Magnitudes for the local sequence stars identified in the field of SN 2003cg coded as in Figure 1.

star	U	B	V	R	I	J	H	K
1	17.15 ± 0.01	16.04 ± 0.01	14.97 ± 0.01	14.27 ± 0.01	13.73 ± 0.01	13.18 ± 0.03	12.63 ± 0.02	12.45 ± 0.01
2	17.39 ± 0.01	17.46 ± 0.01	16.85 ± 0.01	16.49 ± 0.01	16.08 ± 0.01	-	-	-
3	18.43 ± 0.02	17.32 ± 0.01	16.14 ± 0.01	15.37 ± 0.01	14.69 ± 0.01	14.00 ± 0.04	13.26 ± 0.04	13.11 ± 0.03
4	16.96 ± 0.01	16.67 ± 0.01	15.91 ± 0.01	15.47 ± 0.01	15.03 ± 0.01	14.63 ± 0.03	14.10 ± 0.03	13.98 ± 0.04
5	19.70 ± 0.03	18.55 ± 0.01	17.09 ± 0.01	16.18 ± 0.00	15.27 ± 0.02	-	-	-
6	20.54 ± 0.07	19.52 ± 0.01	18.07 ± 0.01	17.18 ± 0.02	16.41 ± 0.02	-	-	-
7	13.70 ± 0.01	13.75 ± 0.01	13.25 ± 0.01	12.88 ± 0.01	12.55 ± 0.02	-	-	-
8	17.56 ± 0.01	17.29 ± 0.01	16.52 ± 0.01	16.13 ± 0.01	15.69 ± 0.01	-	-	-
9	16.41 ± 0.01	16.34 ± 0.01	15.61 ± 0.01	15.19 ± 0.01	14.75 ± 0.01	14.26 ± 0.02	13.77 ± 0.01	13.67 ± 0.02
10	18.22 ± 0.01	18.32 ± 0.01	17.79 ± 0.01	17.48 ± 0.01	17.10 ± 0.01	16.74 ± 0.04	16.48 ± 0.02	16.37 ± 0.01
11	-	21.18 ± 0.01	19.57 ± 0.02	18.24 ± 0.01	16.41 ± 0.01	15.08 ± 0.03	14.48 ± 0.03	14.21 ± 0.04
12	18.08 ± 0.01	17.95 ± 0.01	17.28 ± 0.01	16.90 ± 0.01	16.54 ± 0.01	16.21 ± 0.03	15.85 ± 0.01	15.85 ± 0.04
13	19.73 ± 0.01	18.41 ± 0.01	17.16 ± 0.01	16.37 ± 0.01	15.75 ± 0.01	-	-	-
14	14.67 ± 0.02	14.46 ± 0.01	14.27 ± 0.01	14.12 ± 0.01	13.98 ± 0.01	-	-	-
15	18.70 ± 0.01	17.42 ± 0.01	16.05 ± 0.01	15.19 ± 0.01	14.32 ± 0.01	-	-	-

Table 3. Original near-IR photometry of SN 2003cg.

Date	MJD	Phase* (days)	J	H	K	Instr.
25/03/03◁	52723.06	-6.4	13.71 ± 0.04	13.68 ± 0.05	13.50 ± 0.01	Sofi
28/03/03◁	52726.05	-3.4	13.56 ± 0.08	13.61 ± 0.10	13.42 ± 0.01	Sofi
10/04/03◁	52739.96	10.5	15.18 ± 0.01	14.03 ± 0.01	13.90 ± 0.02	Sofi
12/04/03◁	52741.98	12.5	15.24 ± 0.12	13.92 ± 0.10	13.75 ± 0.01	Sofi
20/04/03◁	52749.17	19.7	14.89 ± 0.17	13.66 ± 0.01	13.59 ± 0.01	Sofi
24/04/03◁	52753.18	23.7	14.76 ± 0.13	13.61 ± 0.03	13.51 ± 0.02	Sofi
01/05/03◁	52760.03	30.6	14.49 ± 0.01	13.83 ± 0.02	13.82 ± 0.02	Sofi
09/05/03◁	52768.98	39.5	15.15 ± 0.09	14.26 ± 0.10	14.34 ± 0.09	Sofi
28/05/03◁	52787.95	58.5	16.55 ± 0.08	15.08 ± 0.01	15.11 ± 0.02	Sofi
16/04/04◁	53110.67	381.2	19.80 ± 0.81	19.00 ± 0.51	20.48 ± 0.69	Isaac
18/05/04◁	53143.01	413.5	20.09 ± 0.21	19.29 ± 0.13	20.55 ± 0.32	Isaac

* Relative to B_{max} (MJD=52729.40)

◁ Photometric night

Sofi = ESO NTT + Sofi 0.29''/px; Isaac = ESO VLT-UT1 + Isaac 0.15''/px

Table 4. Optical spectroscopy of SN 2003cg.

Date	MJD	Phase* (days)	Range (Å)	Instr.
22/03/03	52720.99	-8.5	4227-6981	WHT
23/03/03	52721.89	-7.6	3700-9350	CAF
24/03/03	52722.56	-6.9	3650-9132	SSO
25/03/03	52723.45	-6.0	3720-9153	SSO
26/03/03	52724.89	-4.6	3650-9350	ASI
29/03/03	52727.06	-2.4	4000-7773	ASI
29/03/03	52727.60	-1.9	4000-8500	BAO
30/03/03	52728.90	-0.6	3750-9196	CAF
01/04/03	52730.90	1.4	3900-9350	ASI
04/04/03	52733.90	4.4	3500-7968	TGD
07/04/03	52736.87	7.4	3700-7752	ASI
10/04/03	52739.08	9.6	3380-7970	TGD
11/04/03	52740.89	11.4	3400-8050	TGD
12/04/03	52741.86	12.4	3400-9250	CAF
16/04/03	52745.90	16.4	3500-9250	INT
19/04/03	52748.88	19.4	3800-8050	INT
23/04/03	52752.91	23.4	3800-7750	INT
23/04/03	52752.92	23.5	3800-7750	ASI
26/04/03	52755.89	26.4	3800-9350	CAF
28/04/03	52758.00	28.5	4250-7750	INT
08/05/03	52767.89	38.4	4000-7770	ASI
09/05/03	52768.37	38.9	6100-8920	SSO
13/05/03	52772.93	43.5	3810-9250	INT
22/05/03	52781.97	52.5	3500-8050	TGD
19/04/04	53114.08	384.6	4000-8050	FOR

* Relative to B_{max} (MJD=52729.40)

WHT = William Herschel Telescope + ISIS; CAF = Calar Alto 2.2m + CAFOS; SSO = Siding Spring Observatory 2.3m + Double Beam Spectrograph; ASI = Asiago 1.82m Copernico Telescope + AFOSC; BAO = Beijing Astronomical Observatory 0.85m + CCD; TGD = Telescopio Nazionale Galileo + DOLORES; INT = Isaac Newton Telescope + IDS; FOR = ESO VLT-UT2 + FORS1

1994D (Patat et al. 1996), 1996X (Salvo et al. 2001), 2002bo (Benetti et al. 2004), 2002dj (Pignata et al. in preparation) and 2004eo (Pastorello et al. in preparation). For the early-time NIR corrections we used the extensive spectral sequences of SN 2002bo (Benetti et al. 2004) together with the spectra of SN 2003cg. NIR S-corrections at nebular epochs were not computed owing to the lack of contemporary IR spectra.

Once the synthetic magnitudes for each instrumental setup were obtained, we fitted a low order polynomial to the differences between these and those of the standard system passbands in order to correct for the non-stellar nature of the SN spectra. Some dispersion in the S-corrections relative to a given instrument, resulted from flux calibration errors in the input observed spectra plus the fact that we used spectra from different SNe. Assuming that for each instrument the S-correction changed smoothly with time, we calculated the r.m.s. deviation with respect to the polynomial fit and used this as an estimate of the S-correction errors.

The S-corrections for SN 2003cg in the BVRI bands at early times is generally small (≤ 0.09), as seen in Table 6 and in Figure 2 (top). The 0.85m Beijing telescope data were not

Table 5. Infrared spectroscopy of SN 2003cg.

Date	MJD	Phase* (days)	Range (Å)	Instr.
25/03/03	52723.14	-6.5	7970-24984	Sofi+UKI
27/03/03	52725.35	-4.1	14002-25035	UKI
28/03/03	52726.02	-3.5	9367-24980	Sofi
04/04/03	52733.42	3.9	14242-25030	UKI
14/04/03	52743.40	13.9	10378-25037	UKI
20/04/03	52749.10	19.6	9405-24990	Sofi
21/04/03	52750.23	20.8	9400-25000	Sofi
24/04/03	52753.28	23.8	10381-25033	UKI
30/04/03	52760.10	30.5	9398-24990	Sofi
10/05/03	52769.60	40.1	9397-24990	Sofi

* Relative to B_{max} (MJD=52729.40)

Sofi = ESO NTT + Sofi; UKI = United Kingdom Infrared Telescope + CGS4

S-corrected since it was not possible to find the basic information needed to calculate the global response. Nonetheless, the BAO data are in good agreement with the S-corrected data from other instruments as can be seen in Figure 7. Our S-correction values are comparable to those obtained by Pignata et al. (2004a) for other SNe Ia observed with the same instruments the largest corrections being those in the I band. As in Pignata et al. (2004a), the WFI filter passbands differ from the standard ones by more than do any other instruments.

The central panel of Figure 2 shows the S-correction estimated for the SN 2003cg BVRI magnitudes from 200 to 450 days after B maximum. This work represents one of only a few examples where the S-correction has been computed at late phases. As Pignata (2004b) has already discussed, these corrections are generally larger than around maximum light, especially in the B band. In fact, at late epochs the SNe Ia emit most of their flux in a few strong emission lines and so even small shifts in the filter passbands can produce significant variations in the instrumental magnitudes. We find evidence of dispersion in the late-time S-correction due to the low signal-to-noise ratio of the spectra and to residual galaxy background contamination, but there are no trends in the corrections for each instrument and therefore we have adopted an average constant value.

Table 7 and Figure 2 (bottom) contain the NIR S-corrections for Sofi. We used the same method as described above to place the magnitudes on the standard system of Persson et al. (1998). As we have mentioned before, to determine the colour terms we used the synthetic photometry of Vega, Sirius and the Sun. The corrections were, in general, quite small for SN 2003cg in JK but increased to about 0.13 magnitudes for the H band.

In Tables 1 & 3 we present the supernova magnitudes. These have only been first-order corrected using the colour equation of the instruments. However, in the rest of the paper the magnitudes used have been fully S-corrected as detailed in Tables 6 & 7.

Table 6. Optical S-correction to be added to the data in Table 1, in order to convert the SN magnitudes to the Bessell (1990) system.

date	MJD	Phase* (days)	B	V	R	I	Instr. ¹
23/03/03	52721.94	-7.5	-0.002(± 0.010)	-0.041(± 0.006)	0.006(± 0.001)	-0.065(± 0.003)	CAF
24/03/03	52722.54	-6.9	-0.015(± 0.008)	0.005(± 0.003)	-0.006(± 0.005)	-0.006(± 0.002)	SSO
25/03/03	52723.44	-6.0	-0.015(± 0.008)	0.006(± 0.003)	-0.006(± 0.005)	-0.007(± 0.002)	SSO
26/03/03	52724.82	-4.7	-0.015(± 0.004)	0.006(± 0.009)	-0.016(± 0.005)	0.000(± 0.009)	ASI
27/03/03	52725.85	-3.6	-0.016(± 0.004)	0.003(± 0.009)	-0.016(± 0.005)	0.002(± 0.009)	ASI
28/03/03	52726.02	-3.5	-0.064(± 0.010)	-0.042(± 0.009)	0.012(± 0.008)	-0.014(± 0.007)	WFI
29/03/03	52727.02	-2.5	-0.016(± 0.004)	-0.001(± 0.009)	-0.016(± 0.005)	0.003(± 0.009)	ASI
01/04/03	52730.83	1.4	-0.016(± 0.004)	-0.011(± 0.009)	-0.014(± 0.005)	0.010(± 0.009)	ASI
02/04/03	52731.16	1.7	-0.064(± 0.010)	-0.026(± 0.009)	0.011(± 0.008)	0.012(± 0.007)	WFI
04/04/03	52733.12	3.7	-0.064(± 0.010)	-0.020(± 0.009)	0.009(± 0.008)	0.021(± 0.007)	WFI
04/04/03	52733.89	4.4	-0.004(± 0.006)	-0.050(± 0.008)	-0.020(± 0.002)	-0.042(± 0.005)	TGD
07/04/03	52736.80	7.3	-0.018(± 0.004)	-0.024(± 0.009)	-0.013(± 0.005)	0.021(± 0.009)	ASI
09/04/03	52738.90	9.4	0.001(± 0.006)	-0.039(± 0.008)	-0.021(± 0.002)	-0.027(± 0.005)	TGD
11/04/03	52740.87	11.4	0.002(± 0.006)	-0.036(± 0.008)	-0.021(± 0.002)	-0.022(± 0.005)	TGD
12/04/03	52741.90	12.4	-0.031(± 0.010)	-0.020(± 0.006)	0.009(± 0.001)	0.012(± 0.003)	CAF
14/04/03	52743.07	13.6	-0.067(± 0.010)	0.006(± 0.009)	-0.005(± 0.008)	0.052(± 0.007)	WFI
15/04/03	52744.02	14.6	-0.068(± 0.010)	0.008(± 0.009)	-0.007(± 0.008)	0.054(± 0.007)	WFI
16/04/03	52745.08	15.6	-0.068(± 0.010)	0.010(± 0.009)	-0.009(± 0.008)	0.057(± 0.007)	WFI
17/04/03	52746.09	16.6	-0.069(± 0.010)	0.013(± 0.009)	-0.011(± 0.008)	0.059(± 0.007)	WFI
18/04/03	52747.11	17.6	-0.069(± 0.010)	0.014(± 0.009)	-0.013(± 0.008)	0.060(± 0.007)	WFI
19/04/03	52748.04	18.6	-0.070(± 0.010)	0.016(± 0.009)	-0.015(± 0.008)	0.062(± 0.007)	WFI
20/04/03	52749.07	19.6	-0.070(± 0.010)	0.018(± 0.009)	-0.017(± 0.008)	0.064(± 0.007)	WFI
21/04/03	52750.14	20.7	-0.071(± 0.010)	0.020(± 0.009)	-0.019(± 0.008)	0.066(± 0.007)	WFI
21/04/03	52750.98	21.5	-0.071(± 0.010)	0.021(± 0.009)	-0.021(± 0.008)	0.067(± 0.007)	WFI
23/04/03	52752.01	22.5	-0.072(± 0.010)	0.023(± 0.009)	-0.023(± 0.008)	0.068(± 0.007)	WFI
23/04/03	52752.95	23.5	-0.049(± 0.004)	-0.041(± 0.009)	-0.011(± 0.005)	0.046(± 0.009)	ASI
24/04/03	52753.19	23.7	-0.072(± 0.010)	0.024(± 0.009)	-0.025(± 0.008)	0.069(± 0.007)	WFI
25/04/03	52754.01	24.5	-0.073(± 0.010)	0.025(± 0.009)	-0.027(± 0.008)	0.070(± 0.007)	WFI
25/04/03	52755.00	25.5	-0.073(± 0.010)	0.026(± 0.009)	-0.029(± 0.008)	0.071(± 0.007)	WFI
26/04/04	52755.85	26.4	-0.069(± 0.010)	-0.006(± 0.006)	0.012(± 0.001)	-0.108(± 0.003)	CAF
27/04/03	52756.11	26.6	-0.074(± 0.010)	0.027(± 0.009)	-0.031(± 0.008)	0.072(± 0.007)	WFI
28/04/03	52757.00	27.5	-0.074(± 0.010)	0.028(± 0.009)	-0.032(± 0.008)	0.073(± 0.007)	WFI
30/04/03	52759.13	29.7	-0.075(± 0.010)	0.030(± 0.009)	-0.036(± 0.008)	0.075(± 0.007)	WFI
02/05/03	52761.15	31.7	-0.076(± 0.010)	0.030(± 0.009)	-0.039(± 0.008)	0.076(± 0.007)	WFI
02/05/03	52761.99	32.5	-0.077(± 0.010)	0.031(± 0.009)	-0.040(± 0.008)	0.076(± 0.007)	WFI
04/05/03	52763.01	33.5	-0.077(± 0.010)	0.031(± 0.009)	-0.042(± 0.008)	0.077(± 0.007)	WFI
05/05/03	52764.99	35.5	-0.078(± 0.010)	0.031(± 0.009)	-0.044(± 0.008)	0.078(± 0.007)	WFI
07/05/03	52766.01	36.5	-0.078(± 0.010)	0.031(± 0.009)	-0.046(± 0.008)	0.078(± 0.007)	WFI
07/05/03	52766.85	37.4	-0.049(± 0.004)	-0.040(± 0.009)	-0.011(± 0.005)	0.054(± 0.009)	ASI
07/05/03	52766.99	37.5	-0.078(± 0.010)	0.030(± 0.009)	-0.047(± 0.008)	0.078(± 0.007)	WFI
08/05/03	52767.85	38.4	-0.049(± 0.004)	-0.040(± 0.009)	-0.011(± 0.005)	0.055(± 0.009)	ASI
09/05/03	52768.37	38.9	-0.016(± 0.008)	0.003(± 0.003)	-0.003(± 0.005)	0.016(± 0.002)	SSO
22/05/03	52781.94	52.5	0.011(± 0.006)	-0.026(± 0.008)	-0.022(± 0.002)	0.001(± 0.005)	TGD
23/05/03	52782.84	53.4	-0.048(± 0.004)	-0.033(± 0.009)	-0.011(± 0.005)	0.054(± 0.009)	ASI
31/05/03	52790.92	61.5	0.009(± 0.006)	-0.026(± 0.008)	-0.022(± 0.002)	-0.002(± 0.005)	TGO
07/06/03	52797.36	67.9	-0.016(± 0.008)	-0.007(± 0.003)	-0.002(± 0.005)	0.017(± 0.002)	SSO
19/06/03	52809.02	79.6	-0.070(± 0.010)	0.013(± 0.009)	-0.051(± 0.008)	0.086(± 0.007)	WFI
25/06/03	52815.01	85.5	-0.070(± 0.010)	0.013(± 0.009)	-0.051(± 0.008)	0.086(± 0.007)	WFI
20/11/03	52963.20	233.7	0.029(± 0.008)	-0.096(± 0.021)	0.070(± 0.028)	0.097(± 0.097)	ASI
31/01/04	53035.23	305.8	0.162(± 0.027)	0.158(± 0.051)	0.052(± 0.021)	0.102(± 0.023)	TGD
19/04/04	53114.08	384.6	-0.017(± 0.009)	-0.092(± 0.022)	0.073(± 0.024)	0.053(± 0.019)	FOR
07/05/04	53132.97	413.5	-0.017(± 0.009)	-0.092(± 0.022)	0.073(± 0.024)	0.053(± 0.019)	FOR

* Relative to B_{max} (MJD=52729.40)¹ See note to Table 1 for the telescope coding.

3 THE REDDENING PROBLEM

SN 2003cg appears projected into a dust lane of NGC 3169 (Figure 1) and there are a number of indications that reddening is an important issue for this supernova. The

SN 2003cg spectra exhibit strong interstellar Na I D lines at the rest wavelength of the host, plus weaker absorption at the Milky Way rest wavelength (Figure 3). In addition, there is a narrow absorption at $\sim 6282 \text{ \AA}$ not seen in SN Ia spectra (see Figure 3). This feature coincides with a *diffuse inter-*

Table 7. NIR S-corrections to be added to the data in Table 3 in order to convert the SN magnitudes to the Persson et al. (1998) system.

date	MJD	Phase* (days)	J	H	K	<i>Instr.</i> ¹
25/03/03	52723.56	-6.4	0.021(±0.017)	0.090(±0.023)	0.035(±0.019)	Soff
28/03/03	52726.55	-3.4	0.016(±0.017)	0.074(±0.023)	0.011(±0.019)	Soff
10/04/03	52740.46	10.5	0.024(±0.017)	0.124(±0.023)	-0.017(±0.019)	Soff
12/04/03	52742.48	12.5	0.028(±0.017)	0.131(±0.023)	-0.013(±0.019)	Soff
20/04/03	52749.67	19.7	0.045(±0.017)	0.135(±0.023)	0.011(±0.019)	Soff
24/04/03	52753.68	23.7	0.053(±0.017)	0.123(±0.023)	0.028(±0.019)	Soff
01/05/03	52760.53	30.6	0.063(±0.017)	0.095(±0.023)	0.056(±0.019)	Soff
09/05/03	52769.48	39.5	0.058(±0.017)	0.120(±0.023)	0.077(±0.019)	Soff
28/05/03	52788.45	58.5	0.057(±0.017)	0.120(±0.023)	0.075(±0.019)	Soff

* Relative to B_{max} (MJD=2452729.40)¹ See note to Table 3 for the telescope coding.

stellar band (DIB) measured in e.g. HD 183143 at 6283.86 Å by Herbig (1995). It tends to be seen in the spectra of stars which are heavily obscured and reddened by interstellar dust, and is probably due to a variety of interstellar poly-atomic molecules based on carbon.

Adopting a Virgo distance of 15.3 Mpc (Freedman et al. 2001) and a relative distance from Virgo of 1.18 for NGC 3169 (Kraan-Korteweg 1986), the host galaxy, we estimate a distance modulus for SN 2003cg of $\mu = 31.28$.

Given the observed magnitude at maximum (see Section 4.1), we obtain an absolute V magnitude $M_V^{max} \sim -16.56$ before any reddening correction. This compares with $M_V^{max} = -19.46 \pm 0.05$ for a sample of nearby dereddened SNe Ia sample (Gibson et al. 2000). In addition, the $(B - V)_{max}$ colour is ~ 1.08 redder than typical SNe Ia, which have $(B - V)_{B_{max}} \simeq 0.00 \pm 0.04$ (Schaefer 1995), again pointing to heavy reddening (see Section 4.2).

From these various indicators we conclude that the light emitted by SN 2003cg is heavily reddened. Thus, before discussing the physical properties of the supernova, it is of utmost importance to obtain a precise estimate of the reddening.

3.1 Reddening estimation - Standard procedure

In general, extinction is a function of wavelength. For the V band it is related to the colour excess $E(B-V)$ through the relation,

$$A_V = R_V \times E(B - V), \quad (1)$$

where R_V is the ratio of total-to-selective absorption. Therefore, the problem of estimating the extinction becomes that of measuring the colour excess. Lira (1995) found that the +30–+90 day SN Ia B–V colour curve is identical for all SNe, independent of their light curve and in particular of their $\Delta m_{15}(B)$ (the B magnitude decline between the maximum and 15 days later, Phillips 1993). This indicates an $E(B-V)$ of 1.35 for SN 2003cg. Using the standard value of $R_V = 3.1$, we obtain an intrinsic absolute magnitude of $M_V^{max} \sim -20.91$ cf. the mean $M_V^{max} = -19.46 \pm 0.05$ obtained by Gibson et al. (2000). This implies that either this SN was exceptionally luminous, or that the adopted R_V is too large.

R_V has been well determined in our Galaxy by comparing the colour of reddened and unreddened stars of identical spectral type. Apart from a small dispersion at the shorter wavelengths (Seaton 1979; Savage & Mathis 1979; Cardelli, Clayton & Mathis 1989 (hereafter CCM); O'Donnell 1994; Calzetti 2001), there seems to be a remarkable homogeneity in the optical portion of the interstellar extinction curve along various Galactic directions, with a mean value of $R_V = 3.1$. However, for a few directions values ranging from $R_V = \sim 2$ to ~ 5.5 have been found (Fitzpatrick 2004; Geminal & Popowski 2005). Moreover, we have relatively poor information about the extinction parameters in other galaxies (Chini & Wargau 1990; Jansen et al. 1994; Clayton 2004). In fact, several SNe Ia studies have yielded statistical evidence for lower values of R_V : 0.70 ± 0.33 (Capaccioli et al. 1990), 0.5 (Branch & Tammann 1992), 2.5 ± 0.4 (Phillips et al. 1999), 1.8 (Krisciunas et al. 2000), 2.5 (Knop et al. 2003; Altavilla et al. 2004), 1.55 (Krisciunas et al. 2005), 1.1 and 3.1 (2 components) (Pozzo et al. 2006). Since R_V is related to the characteristics of dust clouds along the line-of-sight, SNe Ia may prove to be a useful probe of the grain properties.

3.2 Reddening estimation - an anomalous extinction law

In order to obtain a precise extinction estimate, we examine more closely the relation between A_λ and $E(B-V)$. CCM provided analytic expressions for the average extinction law A_λ/A_V for the wavelength range $0.125\mu m \leq \lambda \leq 3.5\mu m$. These are characterised by the parameter $R_V = A_V / E(B-V)$. Their analytic formulae reproduce the Galactic mean extinction curve (Seaton 1979; Savage & Mathis 1979) with R_V close to 3.1.

3.2.1 Photometric determination of the extinction

As indicated above, we have estimated the reddening of SN 2003cg using Phillips et al.'s (1999) prescription based on the Lira (1995) result for the late-time B–V colour. We obtain $E(B-V) = 1.35$ (see Table 8). However, in determining the SN 2003cg reddening we would like to make use of

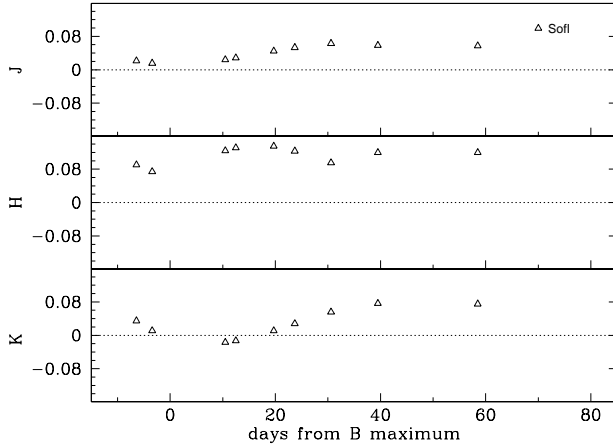
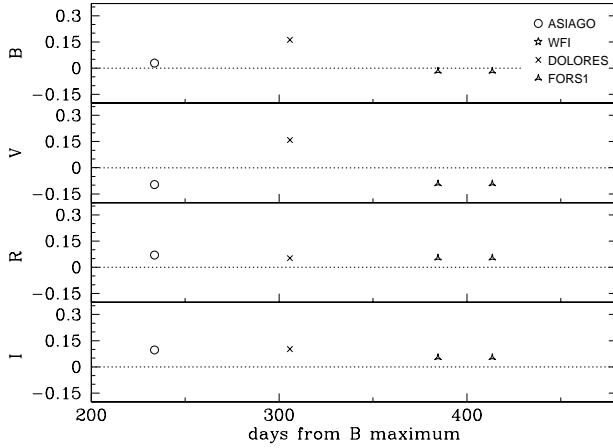
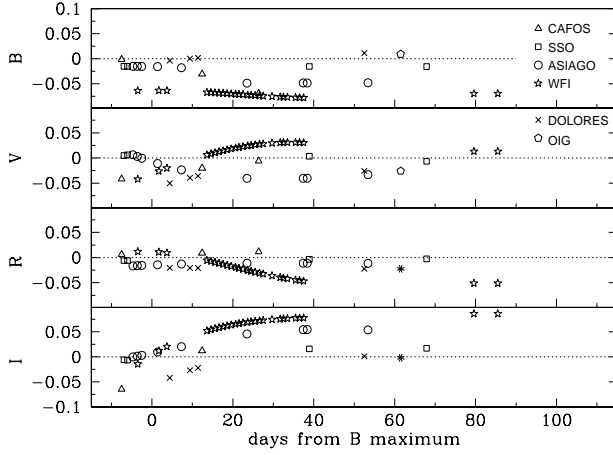


Figure 2. Summary of the S-corrections adopted for the BVRI bands of the different instruments (see legend) at early (top panel) and late (middle panel) times. The early-time S-corrections for the NIR bands are also shown (bottom panel). These corrections should be added to the first-order corrected SN 2003cg magnitudes in order to convert to the standard system values. The dotted line shows the zero correction.

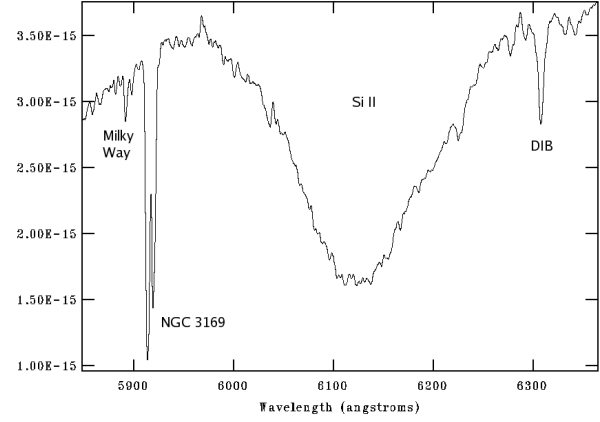


Figure 3. Detail of the interstellar NaID region in the classification spectrum of SN 2004cg obtained on 2003 March 23 with the William Herschel Telescope (+ISIS). The components due to the Galaxy and NGC 3169 are clearly distinguishable. Also visible is a narrow absorption of a DIB at ~ 6282 Å.

most of the colours available, not just (B-V). Therefore, we have compared a range of optical and NIR colour curves of SN 2003cg with those of other normal SNe Ia (Figure 4) (see also Section 4.2). Assuming the CCM absorption law:

$$\frac{A_\lambda}{A_V} = a_\lambda + \frac{b_\lambda}{R_V}, \quad (2)$$

where a_λ and b_λ are wavelength-dependent coefficients, we can write the following expression:

$$E(\lambda_i - \lambda_j) = A_V \left[(a_{\lambda_i} - a_{\lambda_j}) + \frac{b_{\lambda_i} - b_{\lambda_j}}{R_V} \right]. \quad (3)$$

The parameters of this equation were adjusted simultaneously to provide the values of $E(B-V)$ and R_V which gave the best (minimum residual) simultaneous matches to the normal SN Ia colour curves. (cf. Figure 4). This was achieved with $E(B-V) = 1.33 \pm 0.28$ and $R_V = 1.97 \pm 0.29$, clearly a smaller value than the canonical $R_V = 3.1$.

Figure 5 shows the average differences between the observed colours and those expected for $R_V = 3.1$ and $R_V = 2.0$ ($\equiv 1.97$). This plot confirms our result that R_V is small: indeed for $R_V = 2.0$ the residuals are practically zero.

3.2.2 Spectroscopic determination of the extinction

An independent method for determining the extinction is via the equivalent width (EW) of the narrow interstellar NaID doublet. This is believed to be related to the amount of dust between us and the source (Barbon et al. 1990 and Munari & Zwitter 1997). Turatto, Benetti & Cappellaro (2003) studying a sample of SNe Ia, found that the points appear to cluster around two separate relations between EW (NaID) and $E(B-V)$:

$$E(B-V) = 0.16 \times EW(\text{NaID}) \quad (4)$$

$$E(B-V) = 0.51 \times EW(\text{NaID}) \quad (5)$$

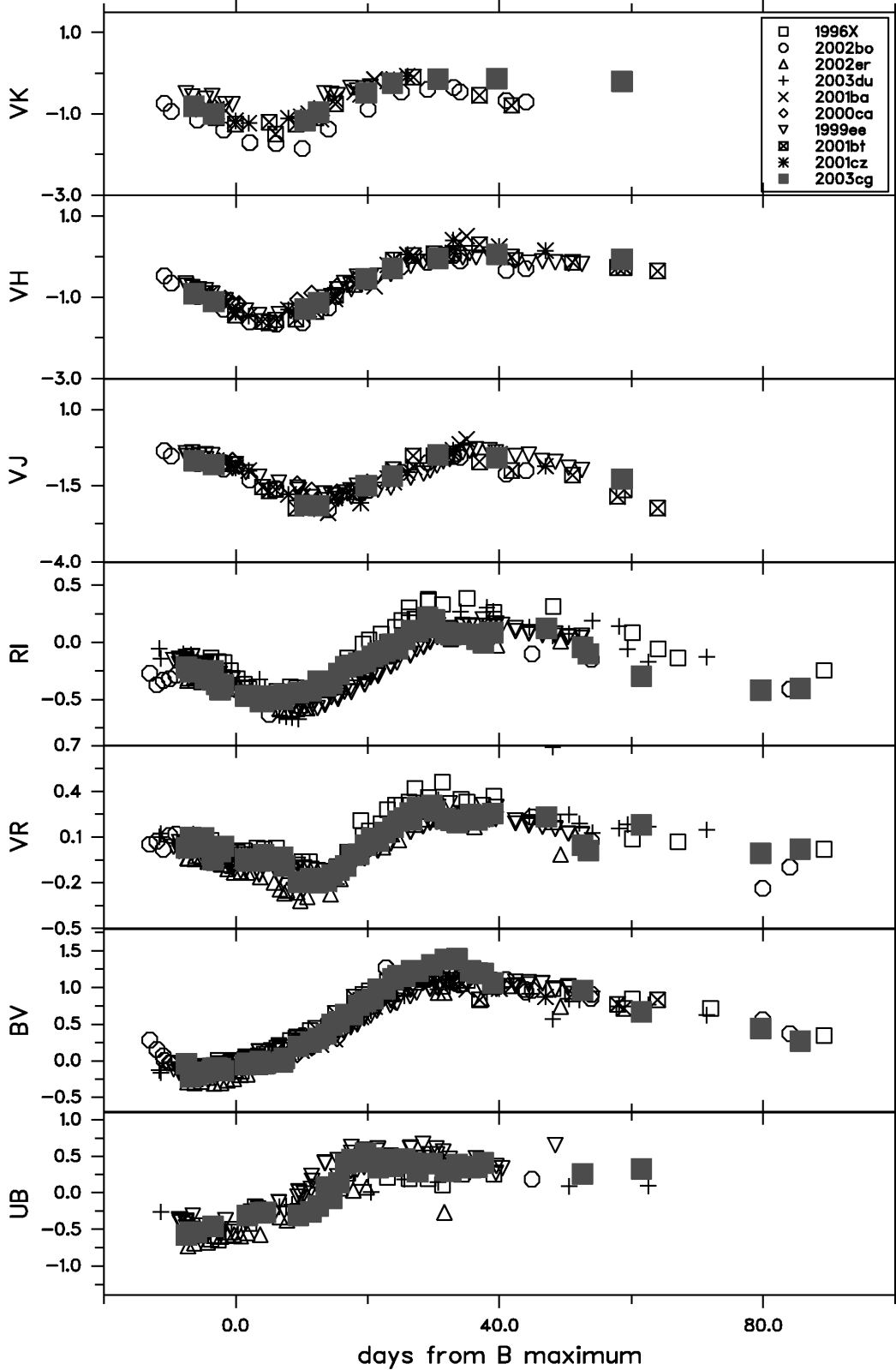


Figure 4. Intrinsic optical and NIR colour curves of SN 2003cg compared with those of SNe 2003du (Stanishev et al. in preparation), 2002er (Pignata et al. 2004a), 2002bo (Benetti et al. 2004; Krisciunas et al. 2004b), 1996X (Salvo et al. 2001), 2001bt, 2001cz (Krisciunas et al. 2004b), 1999ee, 2000ca and 2001ba (Krisciunas et al. 2004a). For a discussion on the reddening adopted, see Section

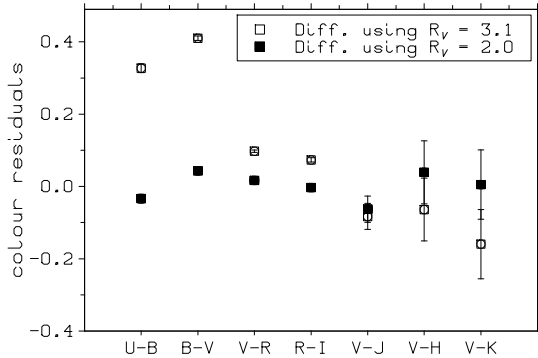


Figure 5. Differences between the observed colour excesses and those computed for $R_V = 3.1$ (empty symbols) and $R_V = 2.0$ (full symbols).

Averaged over the 25 spectra obtained for SN 2003cg, the NaID doublet has an $EW = 0.63 \pm 0.07 \text{ \AA}$ for the Milky Way and $EW = 5.27 \pm 0.50 \text{ \AA}$ for NGC 3169. Using the relations (4) and (5) we find $E(B-V) \sim 0.10$ and $E(B-V) \sim 0.32$ for the Milky Way, and $E(B-V) \sim 0.84$ and $E(B-V) \sim 2.69$ for NGC 3169. The sum of the lower values (from relation 4) for the host galaxy and the Milky Way is 0.94 which is about 0.4 lower than those found in Section 3.2.1. However, since the ratio between the NaID component lines is close to saturation (1.24), we regard this value of $E(B-V)$ as being a lower limit only. We also considered using the EW of the K I (7699Å) absorption line to estimate the reddening (Munari & Zwitter 1997). Unfortunately, the spectra covering this spectral region were of insufficient resolution to detect this much weaker line.

Another way of determining $E(B-V)$ and R_V is to use the optical SED (3400-9350Å) of SN 2003cg. We have developed a script which derives the free parameters of a CCM extinction law by comparison of the SED of SN 2003cg with those of unreddened SNe Ia, at various coeval epochs. The reference SNe were selected to have similar light curve shapes ($\Delta m_{15}(B)$) and spectral features. Their spectra were corrected for redshift and Galactic reddening. The reference spectra were then scaled to the distance of SN 2003cg via:

$$f_{ref}^{03cg} = \left(\frac{d_{ref}}{d_{03cg}}\right)^2 f_{ref}, \quad (6)$$

where f_{ref} is the observed flux of the reference SN at its true distance, d_{ref} , d_{03cg} are the distances of the comparison SN and SN 2003cg respectively and f_{ref}^{03cg} is the flux of the reference SN at the distance of SN 2003cg. The script divides the SN 2003cg spectra by the scaled reference spectra and calculates:

$$A_\lambda = -2.5 \log \frac{f_{03cg}}{f_{ref}^{03cg}}, \quad (7)$$

where A_λ is the total extinction at any wavelength and f_{03cg} is the observed flux of SN 2003cg. Finally, in order to compare with the CCM law (relation 2), we normalise the

derived extinction curve to match the value of A_λ at the V band effective wavelength.

As reference we have used the spectra of SN 1994D ($\Delta m_{15}(B) = 1.26$ - Patat et al. 1996) and SN 1996X ($\Delta m_{15}(B) = 1.31$ - Salvo et al. 2001). We have compared seven pairs of 94D-03cg spectra at different epochs and five pairs of 96X-03cg spectra, obtaining the parameters A_V and R_V in each case. The average values of these parameters for each sets of pairs are given in Table 8. Two examples of this comparison are shown in Figure 6.

From the $E(B-V)$ and R_V values listed in Table 8 (but excluding the NaID measurement) we obtained weighted average values of $E(B-V) = 1.33 \pm 0.11$ and $R_V = 1.80 \pm 0.20$. Using these results we can estimate the NIR colour excesses using the basic relations between A_V , $E(B-V)$ and R_V : $E(V-J) = 1.92$, $E(V-H) = 2.08$ and $E(V-K) = 2.20$. These values are approximately 10% smaller than those we obtained from the comparison of the colour curves reported on Table 11 (see also Section 3.2.1).

Up to this point we have investigated the extinction using methods which either did not involve the value of $\Delta m_{15}(B)$ or where the reference SNe Ia were of similar light curve shape. If a wider diversity of SNe Ia were employed we would have to correct this parameter for the effects of reddening (see Section 4.1.1). Assuming $\Delta m_{15}(B)_{intrinsic} = 1.25$, we checked the $E(B-V)$ using the prescription given by Reindl et al. (2005) at maximum for a sample of 111 "Branch normal" SNe Ia and tentatively for five 1991T-like and +35 days for 59 normal SNe Ia. We obtained for the two epochs $E(B-V) = 1.21 \pm 0.20$ and 1.25 ± 0.11 respectively, which are in excellent agreement with the estimates reported before.

This analysis confirms that the light emitted by SN 2003cg was heavily reddened. However, in order to match its intrinsic luminosity and colour evolution to those of other SNe Ia with similar light curve shapes and spectral features, it was necessary to deredden the SN 2003cg data using a value of $R_V = 1.80 \pm 0.20$. This is significantly less than the standard ISM value of 3.1.

3.3 Effects of a light echo?

Wang (2006) has suggested that the anomalous reddening seen towards a number of SNe Ia may be due to the effects of a dusty circumstellar cloud. In this "light-echo" (LE) scenario, not only is light scattered out of the beam, but also we see light that has been scattered into our line-of-sight. Thus, in addition to the scattering cross-section we also need to consider the (wavelength-dependent) albedo of the grains. Wang finds that a dust cloud of inner radius 10^{16} cm would produce a significant reduction in R_V . However, we suggest that there are a number of difficulties with this scenario. Firstly, the survival of grains at such a small distance from the supernova is rather unlikely. Adopting the bolometric luminosity of SN 2003cg derived below, and scaling from Dwek's (1983) analysis of SN 1979C we find that the inner radius of a dust cloud around SN 2003cg would exceed $\sim 2 \times 10^{17}$ cm. Dust at this large distance would have only a modest effect on R_V (see Wang (2-6) Figure 4). In addi-

tion, a nearby, dusty CSM would be expected to produce other observable effects at later times. By 50–100 days, the fastest-moving ejecta would collide with the CSM producing characteristic spectral features as seen in the peculiar Type Ia SN 2002ic (Hamuy et al. 2003). However, no signs of such an interaction are apparent. Moreover, even if some (larger) grains survived the peak luminosity, their high temperature would produce a strong near-IR excess, as was seen in SN 2002ic (Kotak et al. 2004). However, no normal SN Ia, including SN 2003cg, has shown such an effect. Other LE effects expected but not seen in SN 2003cg, include (a) a reduced $(B - V)$ color range (so, that after matching the colors at maximum, at later phases one would expect the observed color to be bluer than that of a LE-free object), (b) temporal variation in the reddening, (c) an anomalously small Δm_{15} , (d) a significantly brighter late phase tail and (e) broader spectral lines (Patat et al. 2005). We conclude that any circumstellar dust, if present, has only a small effect on the extinction behaviour of SN 2003cg.

We conclude that the small value of R_V for SN 2003cg is most likely due to a grain size distribution where the grains are generally smaller than in the local ISM (Geminale 2006). A more detailed analysis of possible LE effects will be presented in a separate paper.

In the photometric and spectroscopic analysis of SN 2003cg that follows, we adopt $E(B-V) = 1.33 \pm 0.11$ and $R_V = 1.80 \pm 0.20$.

4 PHOTOMETRY

4.1 Light curves

The light curve shape provides one of the main ways by which we acquire information about individual SNe. It is linked directly to the energy input and to the structure of the exploding star. However, it can also be influenced by intervening dust. In the following sections we discuss the early and late light curve phases of SN 2003cg.

4.1.1 Early phase

The optical photometry (Table 1, 6) & and near-IR photometry (Table 3) of SN 2003cg are plotted as light curves in Figure 7. Note in particular the excellent sampling of the optical data from -7 to $+85$ days. Also shown as “ R -band” data are the unfiltered pre-discovery and discovery points of Itagati & Arbour (2003) (see below). In view of the small redshift of SN 2003cg ($z=0.004$), we have not applied K -corrections to any of the magnitudes. The shapes of the light curves are typical of a normal Type Ia SN e.g. (a) the occurrence of secondary maxima longward of the V -band (b) the increased prominence of the secondary maxima in the NIR. Also typical is that maximum light occurred before t_{Bmax} in the U , I and NIR bands, and slightly after in the V and R bands (e.g. Contardo, Leibundgut & Vacca 2000). In order to estimate the maximum light epochs and magnitudes for the different bands, we fitted low order polynomials to the light curves around their respective maxima. The results are given in Table 11 together with

other parameters for SN 2003cg and its host galaxy.

An important light curve width/shape parameter is $\Delta m_{15}(B)$. For SN 2003cg we obtain a direct measurement of $\Delta m_{15}(B) = 1.12 \pm 0.04$. However, the intrinsic light curve shape may be altered by the combined effects of SED evolution and dust extinction. We corrected for this effect using the formula of Phillips et al. (1999) viz. correction = $0.1 \times E(B-V)$. For the $E(B-V)$ derived in the previous section this gives a correction of 0.133 and hence an intrinsic value of $\Delta m_{15}(B) = 1.25 \pm 0.05$. However, in view of the high reddening of SN 2003cg, we decided to check the $\Delta m_{15}(B)$ correction using synthetic magnitudes obtained from its spectra. We computed $\Delta m_{15}(B)$ for (a) the observed spectra and (b) the spectra corrected for Galactic and host galaxy reddening (see Sections 3 and 5). The difference between the two synthetic values is 0.128, very similar to that obtained from the Phillips et al. formula, thus indicating that their formula is valid even at high reddening.

Another useful means of characterising the light curve shape is the stretch factor s (Perlmutter et al. 1997; Goldhaber et al. 2001; Altavilla et al. 2004). This is the factor by which an observed B -band light curve must be expanded or contracted to match a standard light curve shape. We find $s = 0.97 \pm 0.02$ for SN 2003cg, in good agreement with that obtained via the relation $\Delta m_{15}(B) = 1.98 \times (s^{-1} - 1) + 1.13$ (Altavilla et al. 2004).

In Figure 7, for comparison we also plot the light curves of two other nearby Type Ia SNe having similar $\Delta m_{15}(B)$: SN 1994D ($\Delta m_{15}(B) = 1.32$, Phillips et al. 1999) and SN 2002bo ($\Delta m_{15}(B) = 1.13$, Benetti et al. 2004). Both SNe have been: (a) shifted to the SN 2003cg distance (Section 4.3), (b) dereddened according to their colour excesses (0.04 - Phillips et al. 1999 and 0.38 - Stehle et al. 2005 respectively) with $R_V = 3.1$, and (c) artificially reddened with the $E(B-V)$ and R_V values of SN 2003cg (Section 3). We adopt distance moduli of 30.68 and 31.67, for SN 1994D and SN 2002bo, respectively (Patat et al. 1996; Benetti et al. 2004).

With respect to the other two SNe, SN 2003cg has a broader U -band peak. This can be due to the high reddening towards SN 2003cg which shifted the bandpass to redder effective wavelengths where the light curves are broader. The same effect is probably responsible for the pronounced shoulder in the V band light curve which correlates with the emergence of the secondary maxima in the light curves in the R , I and longer wavelength light curves.

SN 1994D and SN 2003cg show similar maximum magnitudes in the UBV bands but in R and I SN 1994D is brighter. In addition, the secondary maximum in I occurs approximately 8 days earlier in SN 1994D. SN 2002bo is approximately 0.5 magnitudes brighter than SN 2003cg in the VRI bands, and approximately 0.5 magnitudes fainter in the U band. In contrast with the optical bands, we find similar behaviour between SN 2003cg and SN 2002bo in the NIR bands (no NIR light curves are available for SN 1994D). We note that the H and K light curve minima of both SN 2002bo and 2003cg occur later and are more pronounced than in the Krisciunas et al. NIR template light curves (Krisciunas et al. 2004a).

As already mentioned (Section 2), SN 2003cg was dis-

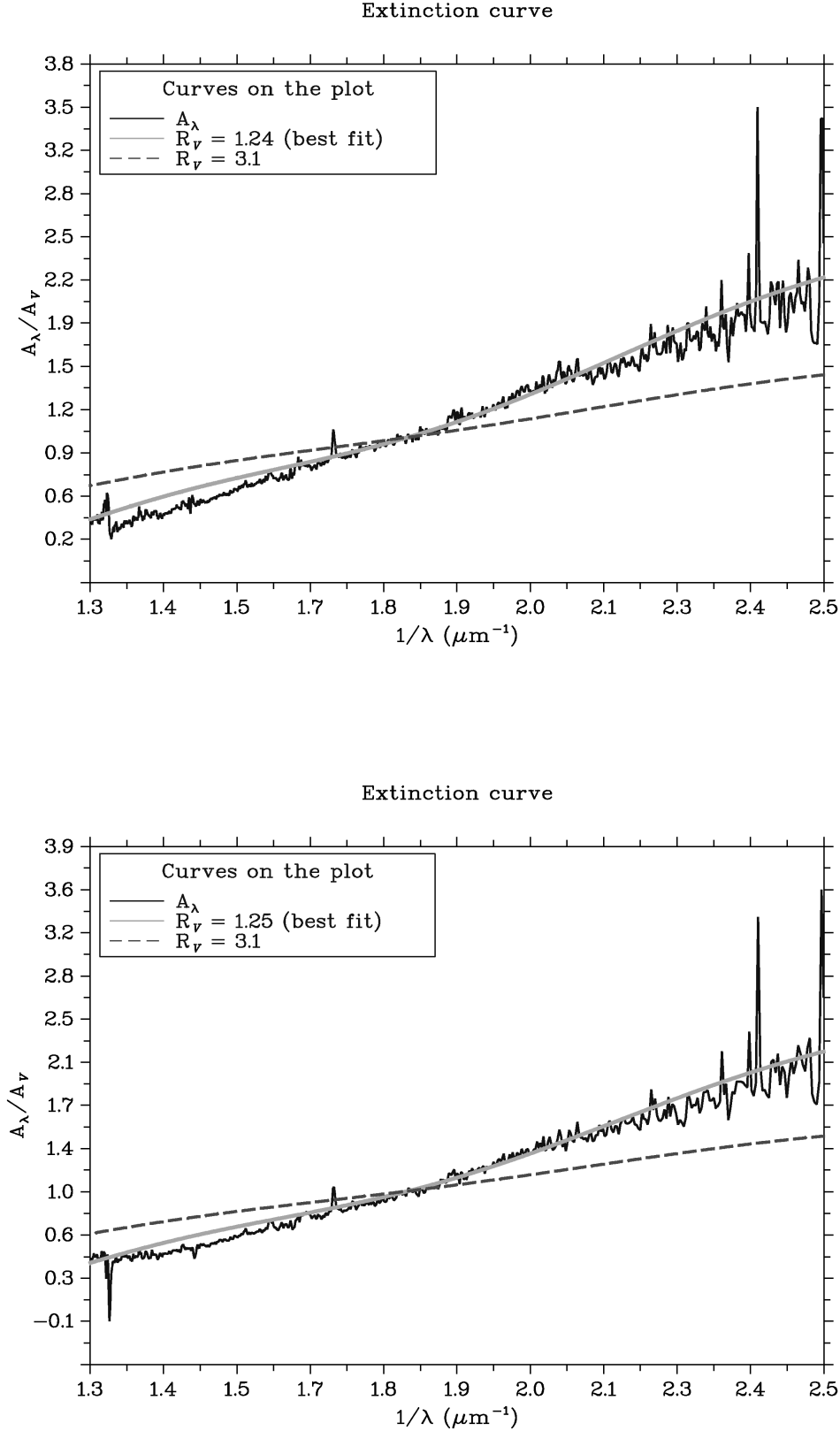


Figure 6. Best fit of theoretical CCM laws (solid line) to empirical extinction curves of SN 2003cg obtained with the pair 1994D-2003cg (top) and 1996X-2003cg (bottom) on day -2. The CCM extinction curve for $R_V = 3.1$ (dashed line) is plotted for comparison.

Table 8. Values of the colour excess and the ratio of total-to-selective extinction derived from different methods.

Method	E(B-V)	R_V	Reference
$E(B-V)_{tail}$	1.35 ± 0.13	–	Phillips et al. (1999)
Colour Evolution	1.33 ± 0.28	1.97 ± 0.29	Section 3.2.1
Comp-CCM (94D)	1.28 ± 0.44	1.61 ± 0.41	Section 3.2.2
Comp-CCM (96X)	1.22 ± 0.33	1.69 ± 0.33	Section 3.2.2
EW of Na I D	0.94	–	Turatto, Benetti & Cappellaro (2003)

covered about 10 days before B maximum. Along with the discovery, Itagati & Arbour (2003) report two unfiltered optical images obtained at -18.1 and -9.1 days (see Table 1). We judge that the magnitudes from these images most closely approximate to those which would have been obtained in the R band (Pignata et al. 2004a).

Riess et al. (1999) suggest that the early ($t_0 \lesssim 10$ days) luminosity is proportional to the square of the time since explosion and derived an estimate of the explosion epoch t_0 . Applying this relationship to the SN 2003cg R band light curve (including the two unfiltered points), we obtain $t_0(R) \lesssim 52709.5 \pm 0.6$ (MJD) i.e. a risetime of 20.4 ± 0.5 days. However, for the B band is $t_r(B) = 19.9 \pm 0.5$ days, significantly longer than that derived by (Riess et al. 1999) (17.71 days) for a SN Ia with a $\Delta m_{15}(B)$ similar to that of SN 2003cg.

4.1.2 Nebular phase

The optical (BVRI) and NIR evolution of SN 2003cg was also monitored at late phases (to over one year post-maximum). The complete light curves, covering both early and late phases, are shown in Figure 8, together with those of SNe 1992A (Suntzeff 1996; Altavilla et al. 2004), 1994D (Patat et al. 1996; Altavilla et al. 2004) and 1996X (Salvo et al. 2001). The evolution of the SN 2003cg optical fluxes is consistent with exponential declines in each band. The decline rates are given in Table 9. The late time optical evolution of the four SNe Ia is broadly similar. The BVRI light curve declines are consistent within the errors with those estimated by Turatto et al. (1990) for SNe Ia. In the NIR, only two points quite close in time are available, and the errors are large. Consequently, little can be said about the NIR decline rate (Table 9).

4.2 Colour curves

We have already demonstrated that SN 2003cg is a heavily extinguished SN Ia. In Section 3 we discussed extensively the reddening of SN 2003cg and the use of the colour as an extinction indicator. In this section we discuss only the intrinsic colour evolution of the supernova.

In Figure 4, the intrinsic colour curves of SN 2003cg (corrected for $E(B-V) = 1.33 \pm 0.11$ and $R_V = 1.80 \pm 0.20$) are compared with those of other SNe Ia (cf. Section 3). The optical colour curves are generally very similar. The most significant difference is in the $(B-V)_0$ colour around $+30^d$ when SN 2003cg presents a redder bump reaching a $(B-V) \sim 1.4$ (see also Figure 9). At maximum, SN 2003cg has $(B-V)_0 \sim -0.28$, and curiously, Phillips et al. (1999) and Jha (2002) found $(B-V)_{Bmax}$ values of -0.09 and -0.10 ,

respectively, for normal SNe Ia (after correction for Galactic and host galaxy extinctions). Consequently, SN 2003cg would stand out from the majority of points on the colour-colour diagram ($(U-B)_{max}$ vs. $(B-V)_{max}$) of SNe Ia shown in figure 3.9 of Jha (2002), and so, in our case, his discussion is not applicable.

The $V-J$, $V-H$ and $V-K$ colour curves of SN 2003cg are also shown in Figure 4 (top panels). Again, the behaviour of SN 2003cg is very similar to that of the comparison sample. In particular, the IR colour evolution of SN 2003cg matches well that of SN 2001bt (Krisciunas et al. 2004b).

In a recent work Wang et al. (2005) introduced the colour parameter, ΔC_{12} , the (B-V) colour measured 12 days after the B maximum. This parameter depends strongly on the decline rate $\Delta m_{15}(B)$ and may provide a means of estimating the reddening due to the host galaxy. They also find a correlation between the peak luminosities of SNe Ia and ΔC_{12} . For SN 2003cg, we measure $\Delta C_{12} = 0.39 \pm 0.11$.

In conclusion we emphasise that, given the reddening derived in Section 3, the intrinsic colour evolution of SN 2003cg is normal over a wide range of wavelengths.

4.3 Absolute magnitudes and the *uvoir* light curve

For a Virgo distance of 15.3 Mpc (Freedman et al. 2001) and a relative distance from Virgo of 1.18 Mpc for NGC 3169 (Kraan-Korteweg 1986), the host galaxy of SN 2003cg, we estimate a distance modulus of $\mu = 31.28$. Using the values for $E(B-V)$ and R_V discussed in Section 3, we obtain $M_B^{max} = -19.26 \pm 0.75$ and $M_V^{max} = -19.06 \pm 0.49$ which is typical for SNe Ia of its $\Delta m_{15}(B)$. We have also used distance-independent parameters to estimate M_B^{max} . In Table 10 we show the SN 2003cg M_B^{max} values derived using peak luminosity v. $\Delta m_{15}(B)$ relations (Hamuy et al. 1996; Phillips et al. 1999; Altavilla et al. 2004; Reindl et al. 2005) scaled to $H_0 = 72 \text{ km s}^{-1} \text{ Mpc}^{-1}$ (Freedman et al. 2001). We also give M_B^{max} obtained from the parameter ΔC_{12} (Wang et al. 2005). The weighted average $M_B^{max} = -19.00 \pm 0.06$ is consistent with the M_B^{max} value obtained from the observed peak magnitude and adopted distance modulus. (M_B^{max} deduced from the Reindl et al. (2005) relation is somewhat discrepant).

A similar comparison using the stretch factor, s , can be made. SN 2003cg has a stretch factor of 0.97 i.e. almost 1, and so we can directly compare its absolute magnitude of $M_B^{max} = -19.26 \pm 0.77$ with the $M_B^{max} = -19.30$ value for $s = 1$ (Nugent, Kim & Perlmutter 2002; Knop et al. 2003). Again the agreement is good.

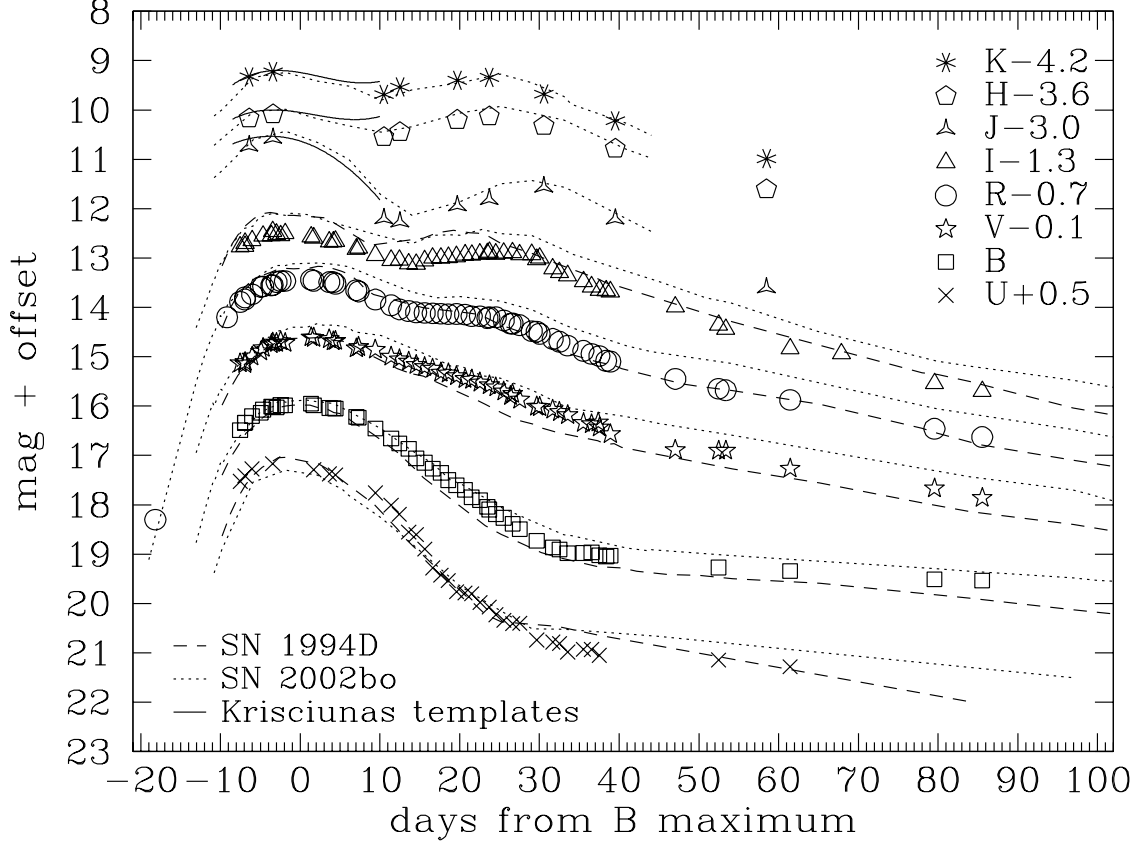


Figure 7. S-corrected optical and IR light curves of SN 2003cg during the first months post-explosion. The light curves have been shifted by the amount shown in the legend. The dashed, dotted and solid lines represent the light curves of SN 1994D (Patat et al. 1996), SN 2002bo (Benetti et al. 2004, Krisciunas et al. 2004b) and JHK templates (Krisciunas et al. 2004a), respectively, adjusted to the SN 2003cg distance and reddening ($E(B-V) = 1.33 \pm 0.11$ and $R_V = 1.80 \pm 0.20$).

Table 9. Decline rates of SN 2003cg at late phases¹.

B	V	R	I	J	H	K
1.40 ± 0.31	1.24 ± 0.14	1.23 ± 0.10	1.99 ± 0.24	0.91 ± 0.51	0.89 ± 0.32	0.22 ± 0.51

¹ Magnitude per 100 days between 233 and 385 days for optical data, and between 381 and 414 for NIR data.

In contrast with the optical region, the IR magnitudes at maximum ($M_J^{max} = -18.23 \pm 0.14$, $M_H^{max} = -17.92 \pm 0.12$ and $M_K^{max} = -17.97 \pm 0.05$) are between 0.4 and 0.5 mag fainter than the values found by Meikle (2000) and Krisciunas et al. (2004b) for two samples of Type Ia SNe.

The "bolometric" (*uvoir*) luminosity evolution of SN 2003cg is shown in Figure 10. It was obtained using the computed distance modulus and reddening, integrating the fluxes in the UBVRIJHK bands (we used a combination of optical and IR spectra having similar epochs) and adding the correction of Suntzeff (1996) for the unknown ultraviolet

contribution. The reddening-corrected bolometric luminosity at maximum is $\log_{10} L = 43.01 \pm 0.05$ (ergs^{-1}). Also shown in Figure 10 are the *uvoir* light curves for five other SNe Ia. The *uvoir* light curve shape of SN 2003cg is clearly similar. In particular, SNe 1996X, 2002er and 2003cg all exhibit prominent bumps around +25 days corresponding to the second NIR maxima. However, SN 2003cg is fainter than SN 1996X around maximum. Differences in the bolometric luminosities at maximum may be due to errors in the distance modulus or reddening estimates for the different SNe.

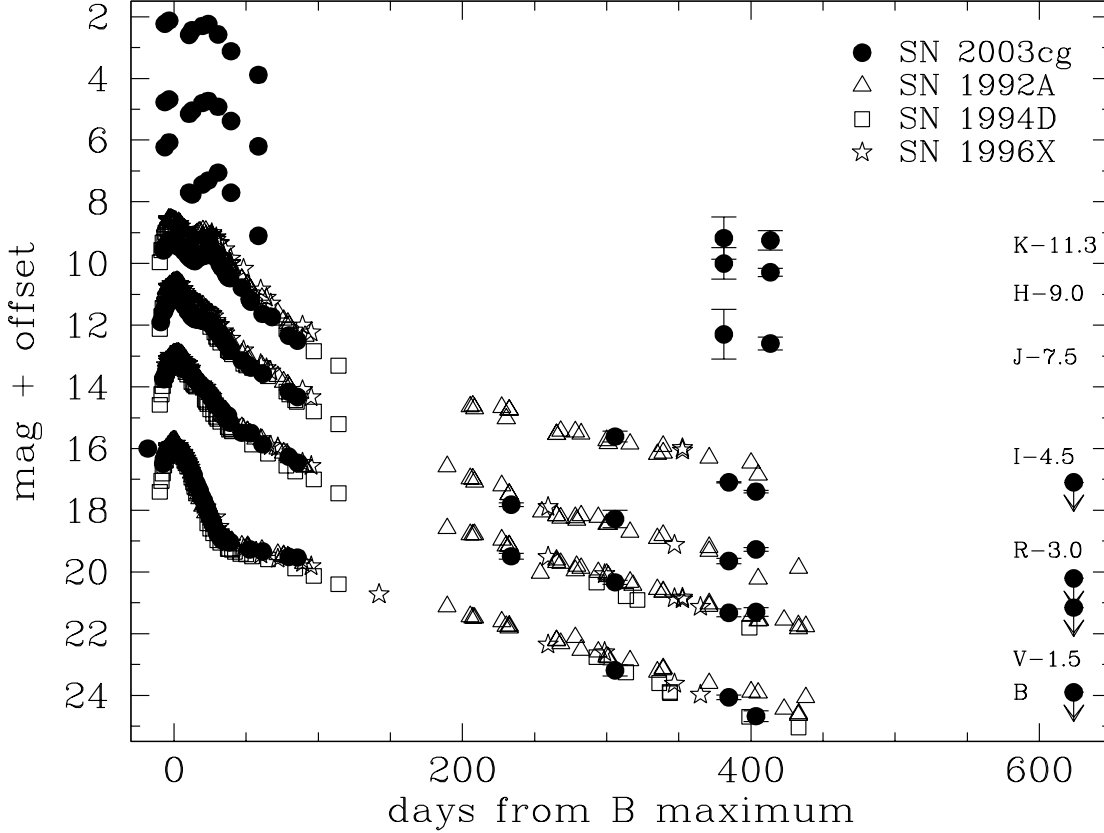


Figure 8. S-corrected BVRIJHK light curves for SN 2003cg covering early and late phases. For clarity, the light curves have been displaced vertically by the amounts shown on the right. Triangles, squares and stars represent the data of SN 1992A (Suntzeff 1996; Altavilla et al. 2004), SN 1994D (Patat et al. 1996; Altavilla et al. 2004) and SN 1996X (Salvo et al. 2001) respectively. They have been adjusted to the SN 2003cg distance and reddening ($E(B-V) = 1.33 \pm 0.11$ with $R_V = 1.80 \pm 0.20$). The lack of data from 3 to 7 months, and from 13 to 20 months is due to seasonal gaps.

5 SPECTROSCOPY

As can be seen in Figure 11, a good set of optical spectra were acquired for SN 2003cg, spanning -8.5 to $+52.5$ days, plus a nebular spectrum taken 384.6 days after B maximum. We also obtained ten early-time NIR spectra (Figure 13) with NTT and UKIRT. This data set constitutes a remarkable sequence of spectra and allows a detailed IR spectroscopic study.

5.1 Optical spectra

Figure 11 shows the optical spectral evolution of SN 2003cg. It is similar to that of other 'normal' Type Ia SNe apart from the red gradient due to the high reddening. Evidence of high extinction towards SN 2003cg is apparent in all the spectra in the form of strong ($EW = 5.27 \pm 0.50 \text{ \AA}$) Na I D interstellar absorption at $\lambda \sim 5915 \text{ \AA}$. Some of the spectra like that at -7.6 day also show interstellar Ca II H & K absorption at $\lambda 3934$ and 3968 \AA . Around maximum light

the spectra show the P Cygni profile of Si II at $\sim 4130 \text{ \AA}$. Also two prominent absorptions are present in SN 2003cg at $\sim 4300 \text{ \AA}$ and at $\sim 4481 \text{ \AA}$. These are attributed to Fe II and Mg II respectively. Fe II blend is again present around 5000 \AA . Between 5958 and 5979 \AA we find Si II and Si III. The earliest Ca II IR triplet spectra include a weak high velocity component. For the -8.5 day spectrum we find $v \sim 22000 \text{ km s}^{-1}$ for this component. The high-velocity feature disappears after maximum light. Mazzali et al. (2005) carried out a detailed study of the high velocity feature in a number of SNe Ia including SN 2003cg.

A single late-phase (nebular) spectrum was secured with the ESO VLT-UT2+FORs1 at $+384.5$ days. A spectrum at this late phase is particularly valuable since the ejecta are mostly transparent to optical/NIR light. Thus, via modelling it is possible to estimate directly the total mass of ^{56}Ni synthesised in the explosion. Mazzali et al. (in

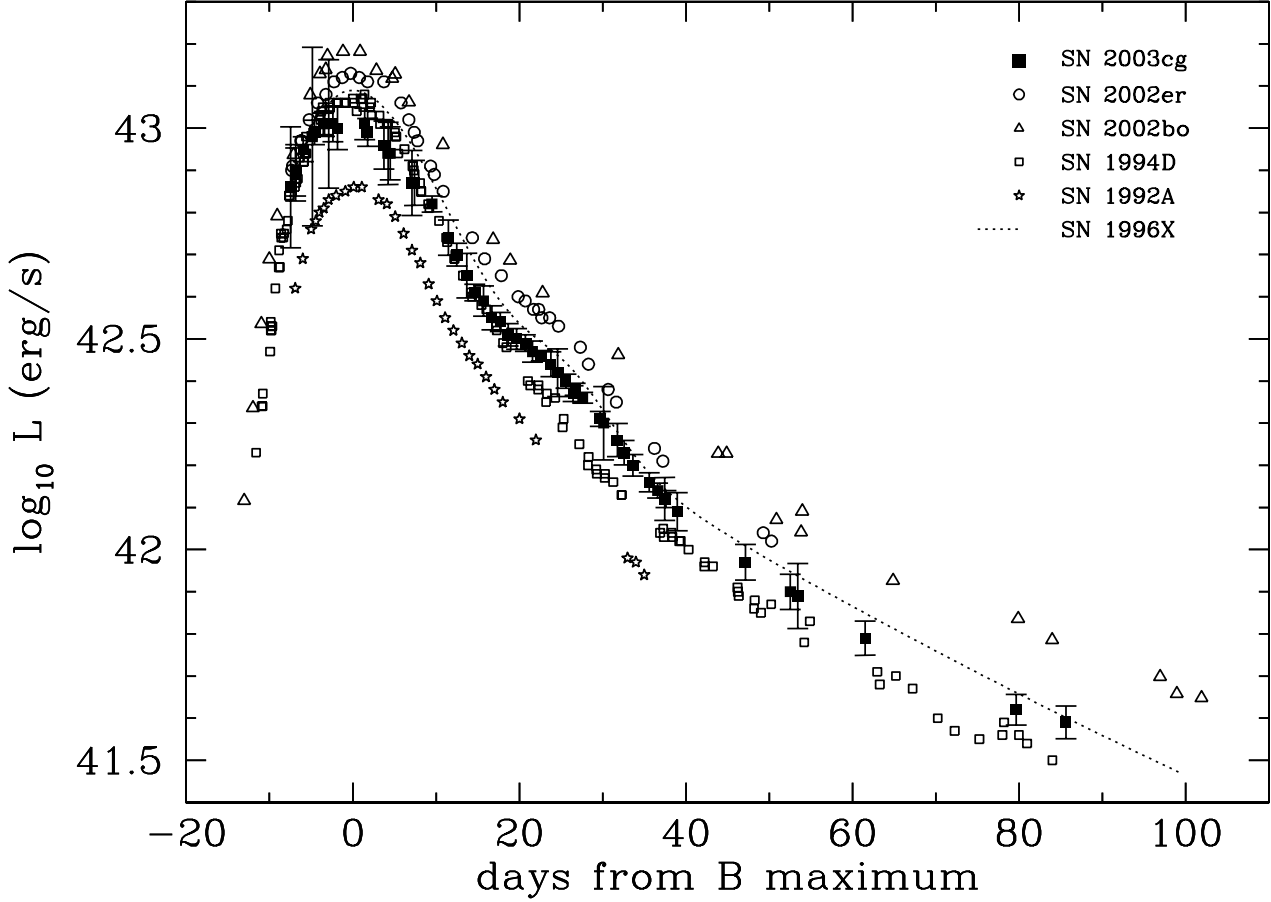


Figure 10. *uvoir* light curve for SN 2003cg. Filled squares give the *uvoir* light curve of SN 2003cg. Dotted line is the *uvoir* light curve for SN 1996X. Open stars, squares, circles and triangles give the *uvoir* light curve for SN 1992A, SN 1994D, SN 2002er and SN 2002bo, respectively. Error bars refer only to photometric errors and not to uncertainties in reddening and distance.

Table 10. Absolute B magnitude of SN 2003cg derived from different methods.

B	Method	Reference
-19.26 ± 0.75	Distance	This work
-18.91 ± 0.13	M_B^{max} vs. $\Delta m_{15}(B)$ ¹	Hamuy et al. (1996) ²
-18.90 ± 0.10	M_B^{max} vs. $\Delta m_{15}(B)$	Phillips et al. (1999)
-19.21 ± 0.12	M_B^{max} vs. $\Delta m_{15}(B)$	Altavilla et al. (2004) ³
-18.22 ± 0.56	M_B^{max} vs. $\Delta m_{15}(B)$	Reindl et al. (2005)
-19.20 ± 0.22	M_B^{max} vs. ΔC_{12}	Wang et al. (2005)

(1) $\Delta m_{15}(B)_{intrinsic}$;

(2) according to the relation given in Table 3 of Hamuy et al. (1996) (peak luminosity);

(3) according to the relation given in Table 1 of Altavilla et al. (2004) ($\Delta Y/\Delta Z=2.5$).

preparation) estimate $M_{Ni} = 0.53 \pm 0.05 M_{\odot}$ for this SN Ia.

In Figure 12 (top) we compare the SN 2003cg optical

spectra around maximum light with those of other SNe Ia such as SNe 2003du (Stanishev et al. in preparation), 2002er (Kotak et al. 2005), 2002bo (Benetti et al. 2004) and 1996X (Salvo et al. 2001). Comparison of the SN 2003cg nebular phase spectrum with those of SNe 2002bo and 1996X is also shown in Figure 12 (bottom). The Δm_{15} values of these SNe Ia are in the range 1.07-1.33, close to the average for SNe Ia. In spite of this relative homogeneity there are some clear differences between the spectra. At maximum light both SN 2003cg and SN 2002er show well-developed, structured features due to intermediate mass elements but with clear differences in the P Cygni profiles until $\sim 4500 \text{ \AA}$. However, the same features in SN 2003du are less pronounced, possibly due to high expansion velocity or composition effects. The SN Ia-defining Si II $\lambda 6355$ line is clearly visible until ~ 28 days after maximum. The line has a fairly symmetrical profile as is also the case for SNe 1996X and 2002er. Somewhat less symmetrical profiles are seen in SNe 2002bo and 2003du. The Si II ($\lambda 6355 \text{ \AA}$) trough blueshifts are similar for SN 2003cg and SN 2003du (see Section 5.3). However the pre-maximum light Ca II H

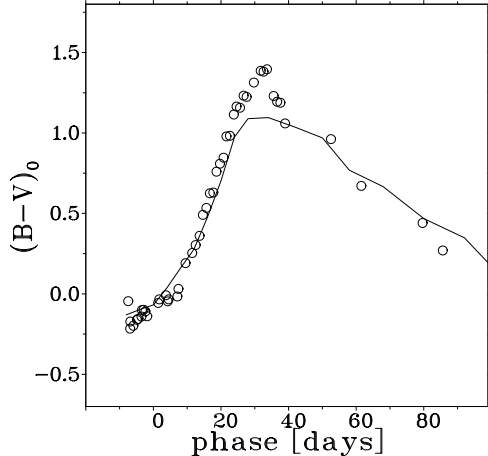


Figure 9. Intrinsic $(B-V)$ colour curve of SN 2003cg (circles) compared with the average $(B-V)_0$ colour curve (solid line) obtained from SNe 2003du (Stanishev et al. in preparation), 2002er (Pignata et al. 2004a), 2002bo (Benetti et al. 2004; Krisciunas et al. 2004b), 1996X (Salvo et al. 2001), 2001bt, 2001cz (Krisciunas et al. 2004b), 1999ee, 2000ca and 2001ba (Krisciunas et al. 2004a). For a discussion on the reddening adopted, see Section 3.2.1.

& K (λ 3934 and 3968 Å) trough blueshifts in SN 2003du are higher by a factor $\sim \times 1.2$ and decline more slowly with time than in SN 2003cg.

In the nebular spectrum of SN 2003cg (Figure 12 - bottom) the $[\text{Fe II}]/[\text{Fe III}]$ emission feature at ~ 4600 Å is comparable to that seen in SN 2002bo but is less pronounced than in SN 1996X. For this feature, the position of SN 2003cg on a plot of FWHM vs. $\Delta m_{15}(B)$ coincides with the average regression curve for SNe Ia. (Mazzali et al. 1998- Figure 2). The $[\text{Co II}]$ 5900 Å emission (Axelrod et al. 1980) appears barely visible above the noise. The boxy feature between 7000 and 7600 Å may be due to a blend of $[\text{Fe II}]$ and $[\text{Ca II}]$ (Figure 12 - bottom).

5.2 Near-infrared spectra

Near-infrared (NIR) spectra are important because there is reduced line blending and lower line opacity. Consequently, line identification is less ambiguous and we may look more deeply into the ejecta. Thus, the line intensities and profiles provide a tool for analysing the ejecta composition and stratification. In Figure 13 we show the NIR spectral evolution of SN 2003cg. The spectral evolution is typical of SNe Ia. The earliest spectra are dominated by continuum emission but, as the photosphere recedes, the spectra are increasingly dominated by discrete, doppler-broadened features. In Figure 14 we compare three early-phase (-6d, +14d, +31d) NIR spectra of SN 2003cg with approximately

coeval spectra of SNe 1994D (Meikle et al. 1996), 1999ee (Hamuy et al. 2002), 2002bo (Benetti et al. 2004) and 2002er (Kotak et al. 2005).

In the pre-maximum spectra of SN 2003cg a weak P Cygni profile is visible at about 10500 Å. This feature was first noted in pre-maximum spectra of SN 1994D by Meikle et al. (1996). This was discussed by Meikle et al. (1996); Mazzali & Lucy (1998); Hamuy et al. (2002); Benetti et al. (2004) and attributed to He I 10830 Å or Mg II 10926 Å. On the basis of their modelling, Meikle et al. (1996) and Mazzali & Lucy (1998) concluded that He I, Mg II or a mixture of the two could be responsible for the feature. In contrast, according to the NIR spectral models of Wheeler et al. (1998), the feature must be due almost entirely to Mg II as there is not enough He in the model atmosphere to form a He line. However, simultaneous optical-IR spectral model fits to SN 1994D by Hatano et al. (1999) and examination of the -7 day spectrum of SN 2002cx by Nomoto et al. (2003) has led these authors to challenge the Mg II identification. They find that the Mg II interpretation also predicts non-existent features at other wavelengths. It is possible that the Mg II explanation is only appropriate for faster decliners. Regardless of which identification we adopt, we find that the trough blueshift of SN 2003cg at -6.5 days is similar to that seen in SN 1994D at -8.5 days.

In the SN 2003cg and SN 1999ee spectra Fe III 12550 Å emission is visible (Figure 14). In addition, a broad P Cygni-like feature is present at ~ 16700 Å. According to Wheeler et al. (1998), this is due to Si II. In the *K*-band, emission at 20500 Å is visible in SN 2003cg. This was also seen in SN 2002bo, albeit more weakly, and was identified with Si III (Benetti et al. 2004).

By +1 to +2 weeks, the weak Mg II/He I ~ 10800 Å absorption has disappeared and strong absorption/emission features have appeared. The prominent emission at 13000 Å is attributed to Si II, while the strong features around 15500-17500 Å are produced by iron group elements such as Co II, Fe II and Ni II (Wheeler et al. 1998). In the *K* band Si II and Fe-group lines have appeared (Wheeler et al. 1998). This indicates that, by this epoch, the NIR photosphere has already receded through the intermediate mass element zones and has penetrated quite deeply into the Fe-group region. In this respect, SN 2003cg is more similar to SN 2002bo than to SN 2002er whose spectrum was more characterised by lighter elements during this era. Like SN 1999ee, SN 2003cg presents spectral features due to Mg, Ca and the Fe-group elements around 12000 Å but at a lower strength.

By one month post-maximum light the three broad emission peaks in the range 21350-22490 Å, produced by Co, Ni and Si, have become more prominent. This is similar to the behaviour seen in other SNe Ia over this spectral range and phase.

Figure 15 shows combined coeval optical and IR spectra of SN 2003cg, allowing a more complete view of the SED evolution. We find that, at -6.5 days the NIR flux (integrated between 10000 and 25000 Å) contribution was about 8% of

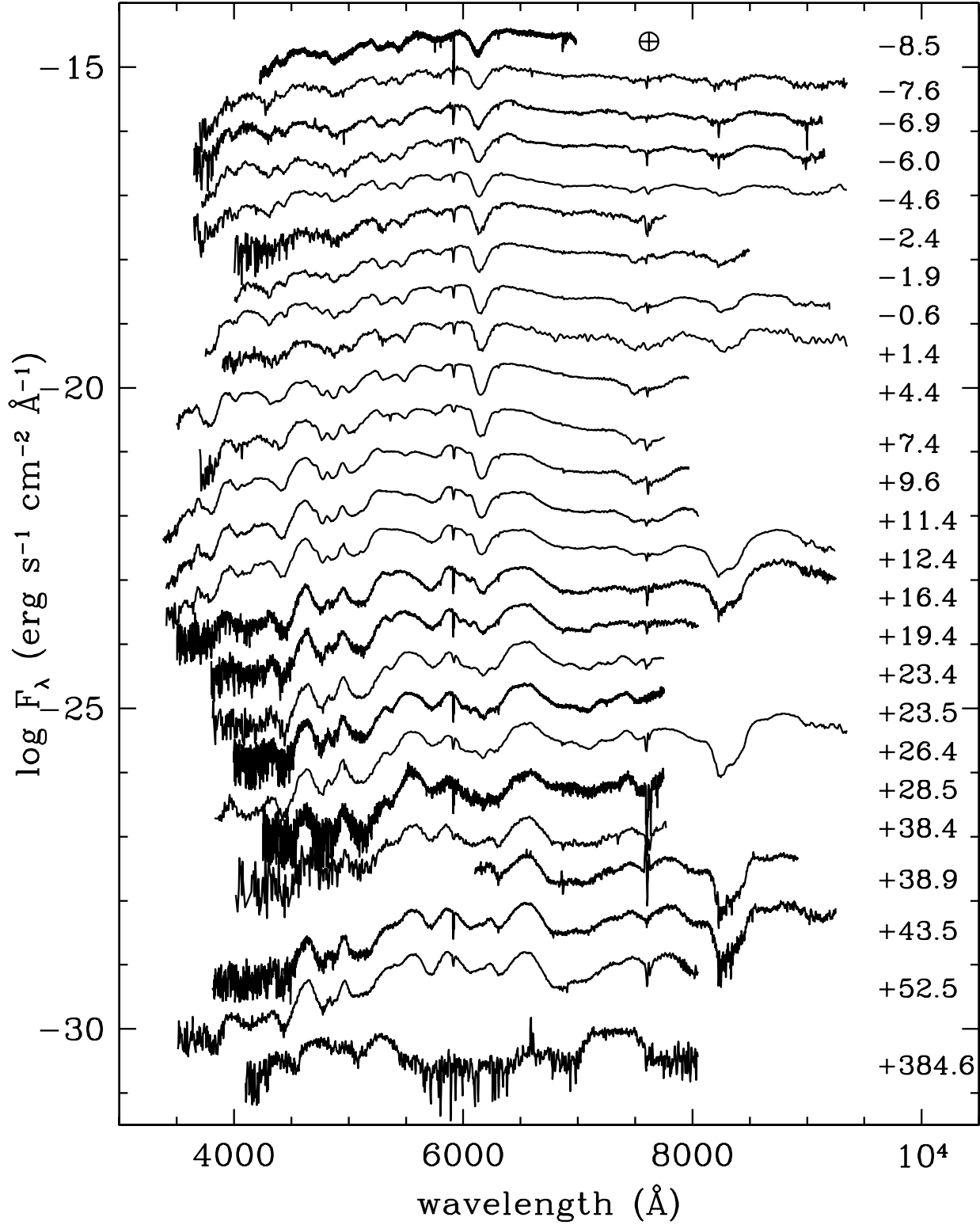


Figure 11. Optical spectral evolution of SN 2003cg. The ordinate refers to the first spectrum and the others have been shifted downwards by arbitrary amounts. Epochs are given at the right hand side. The \oplus indicates the location of the strongest telluric band, which has been removed when possible.

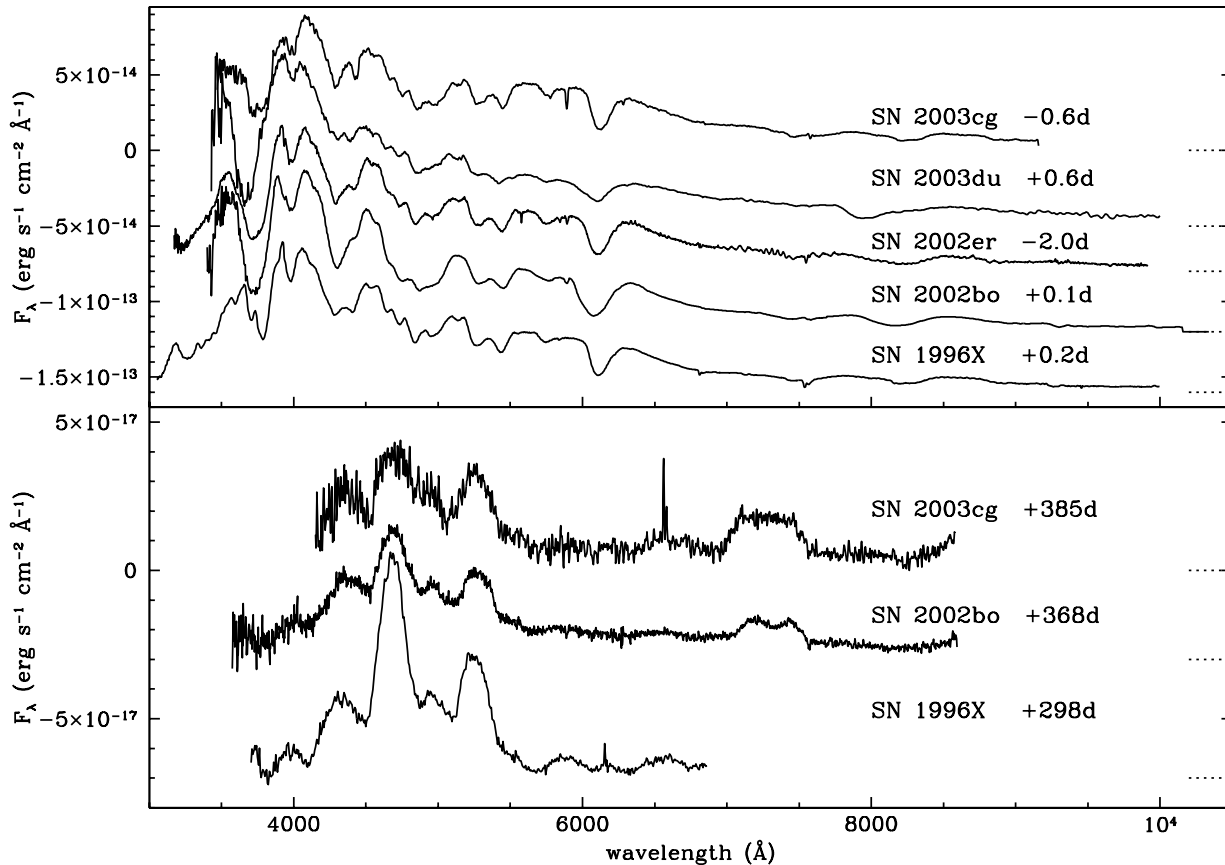


Figure 12. Comparison between optical spectra of SN 2003cg with those of SNe 2003du (Stanishev et al. in preparation), 2002er (Kotak et al. 2005), 2002bo (Benetti et al. 2004) and 1996X (Salvo et al. 2001) at maximum light (top) and at late-phase (bottom). The spectra have been displaced vertically for clarity (the zero-flux levels are indicated by the dotted lines). All the spectra have been corrected for redshift and reddening (see text).

the total flux, rising to about 14% at +23.8 days. For the same interval, Suntzeff (1996, 2003) estimated the contribution of IR in SNe Ia to be approximately 15% of the total flux.

5.3 Velocity Gradient

As can be seen in Figure 11, SN 2003cg exhibits a deep and symmetric Si II trough at 6355 Å, visible approximately from -8 to +28 days, and shifting rapidly redwards with time. In Figure 16, we compare the SN 2003cg Si II velocity evolution with those of a sample of SNe Ia. Clearly, SN 2003cg lies within the low velocity gradient group (hereafter LVG)⁵. The SN 2003cg velocity gradient $\dot{v} \sim 38 \pm 6 \text{ km s}^{-1} \text{ d}^{-1}$ and its expansion velocity at 10 days

past maximum $v_{10}(\text{Si II}) = 10310 \pm 0.10 \text{ km s}^{-1}$. These are typical LVG values. By way of comparison, we also show in Figure 16 the velocity evolutions of the HVG SN 2002bo (HVG) and the FAINT SN 1986G.

In Figure 17 we show the velocity evolution of the Si II 5640 Å trough blueshift, compared with those of three other normal SNe Ia. This feature tends to disappear more quickly than does Si II, and is generally difficult to discern beyond +10 days. SNe Ia show two types of behaviour here, exhibiting either a steep velocity gradient (e.g. SN 2002bo) or a shallow gradient (e.g. SNe 1994D, 2003du) (Benetti 2005). It may be seen that SN 2003cg falls into the latter category.

$\mathcal{R}(\text{Si II})$, the ratio of the depths of the Si II 5972 Å and 6355 Å absorptions, was introduced by Nugent et al. (1995) as a potential distance-independent parameter which is

⁵ Benetti et al. (2005) have analysed the photometric and spectroscopic diversity of 26 SNe Ia. They identify three groups: FAINT (faint SNe Ia with low expansion velocities and rapid evolution of the Si II velocity), HVG ('normal' SNe Ia with high velocity gradients, brighter absolute magnitudes and higher ex-

pansion velocities than the FAINT SNe) and LVG ('normal' and SN 1991T-like SNe Ia with small velocity gradients).

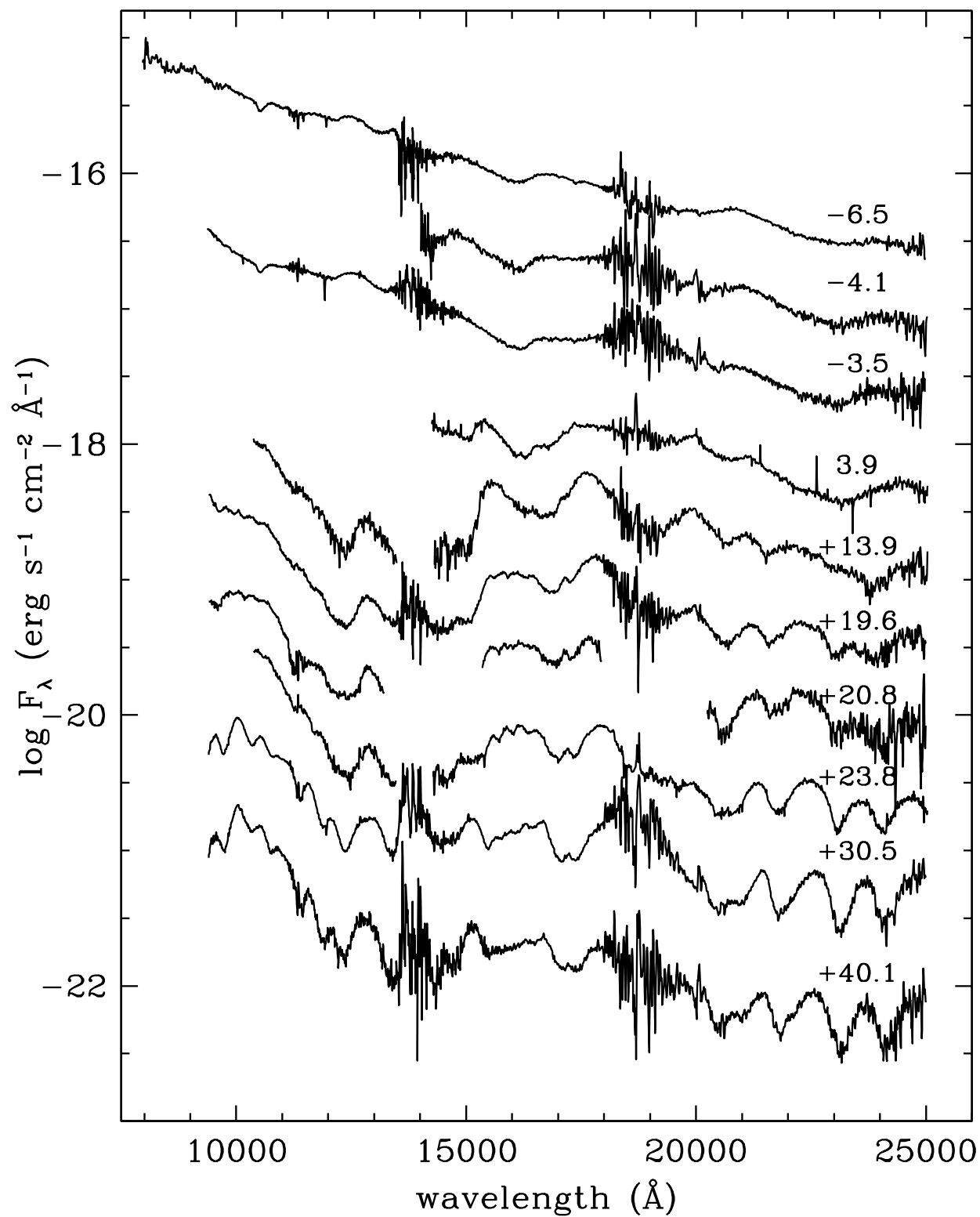


Figure 13. NIR spectral evolution of SN 2003cg. The ordinate refers to the first spectrum and the others have been shifted downwards by arbitrary amounts. Epochs are shown to the right.

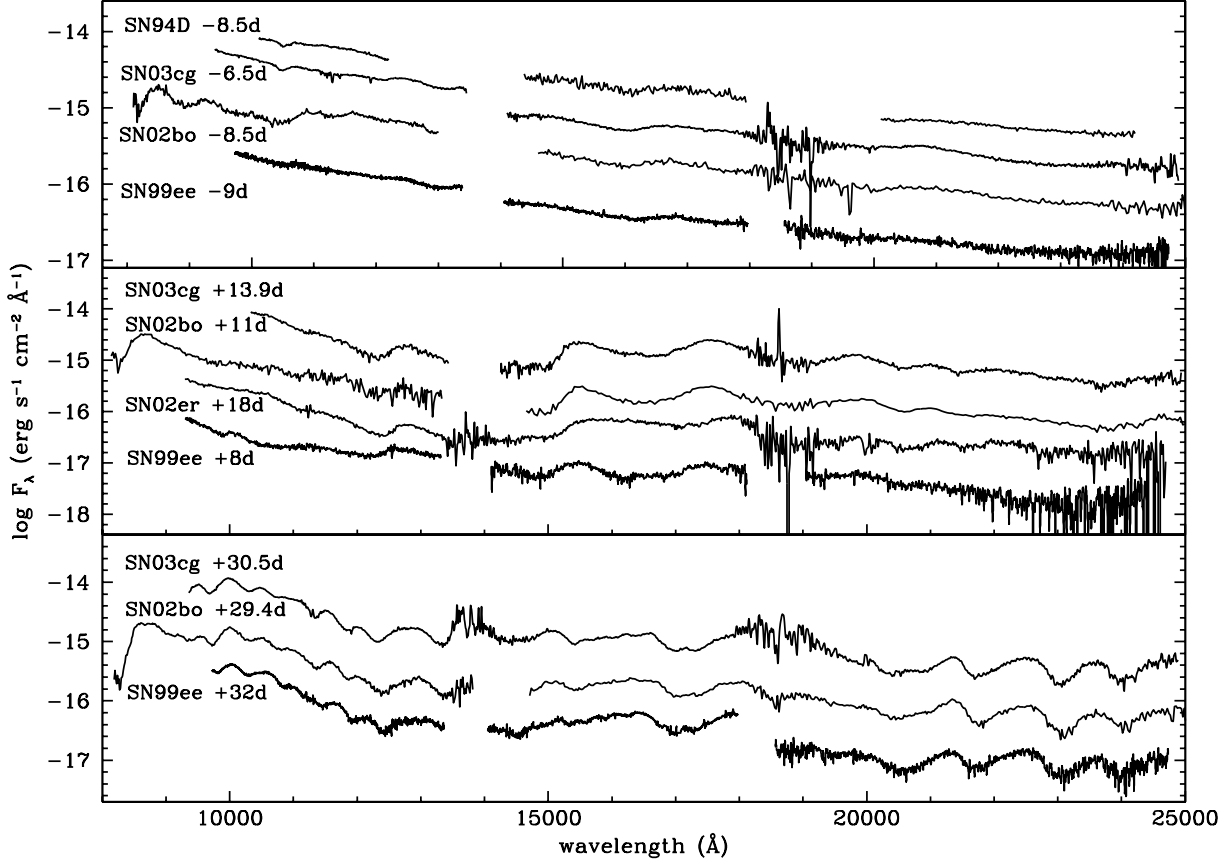


Figure 14. Comparison between the NIR spectra of SN 2003cg and those of SNe 1994D (Meikle et al. 1996), 1999ee (Hamuy et al. 2002), 2002bo (Benetti et al. 2004) and 2002er (Kotak et al. 2005) before maximum (top), two weeks after maximum (middle) and one month after maximum (bottom). The spectra have been displaced vertically for clarity. All spectra have been corrected for reddening (see text) and parent galaxy redshift.

related to the luminosity. The parameter was investigated further by Benetti et al. (2005). For SN 2003cg, $\mathcal{R}(\text{Si II})_{\text{max}} = 0.30 \pm 0.05$. In Figure 18 it may be seen that the pre-maximum evolution of $\mathcal{R}(\text{Si II})$ for SN 2003cg is similar to that of other LVG SNe Ia i.e. little or no pre-maximum evolution occurs.

We repeated the Benetti et al. (2005) cluster analysis including SN 2003cg. We found that this SN does indeed belong to the LVG cluster (see Figure 19). In the five-parameter space ($\Delta m_{15}(\text{B})$, M_B^{max} , \dot{v} , $v_{10}(\text{Si II})$ and $\mathcal{R}(\text{Si II})_{\text{max}}$), the nearest SNe to SN 2003cg are SN 1994D and SN 1996X. This supports our choice of these SNe for comparison purposes in this work.

5.4 Spectral modelling

We have compared the observed spectra of SN 2003cg with synthetic spectra derived using the Lucy-Mazzali Monte Carlo code, which has been used successfully to model spec-

tra of SNe Ia in the photospheric phase (e.g. Mazzali & Lucy 1993). The code (Mazzali & Lucy 1993; Lucy 1999; Mazzali 2000) assumes that the SN ejecta can be separated by a sharp photosphere into an optically thick region below which all the light is emitted and an optically thin region where line formation occurs. The code's input parameters are the SN luminosity, a photospheric velocity (which is equivalent to radius since $v = r/t$), a density structure and a set of abundances. The density structure used here is that of the W7 model (Nomoto, Thielemann & Tokoi 1984). The flux at the photosphere is assumed to be emitted with a black-body spectrum. The code follows the propagation of photons in the ejecta and their interaction with lines (including the process of branching) and electron scattering. Excitation and ionisation are computed using a nebular approximation, which gives a good description of the conditions in a SN Ia near maximum (Pauldrach et al. 1996). The emerging spectrum is computed using a formal integral.

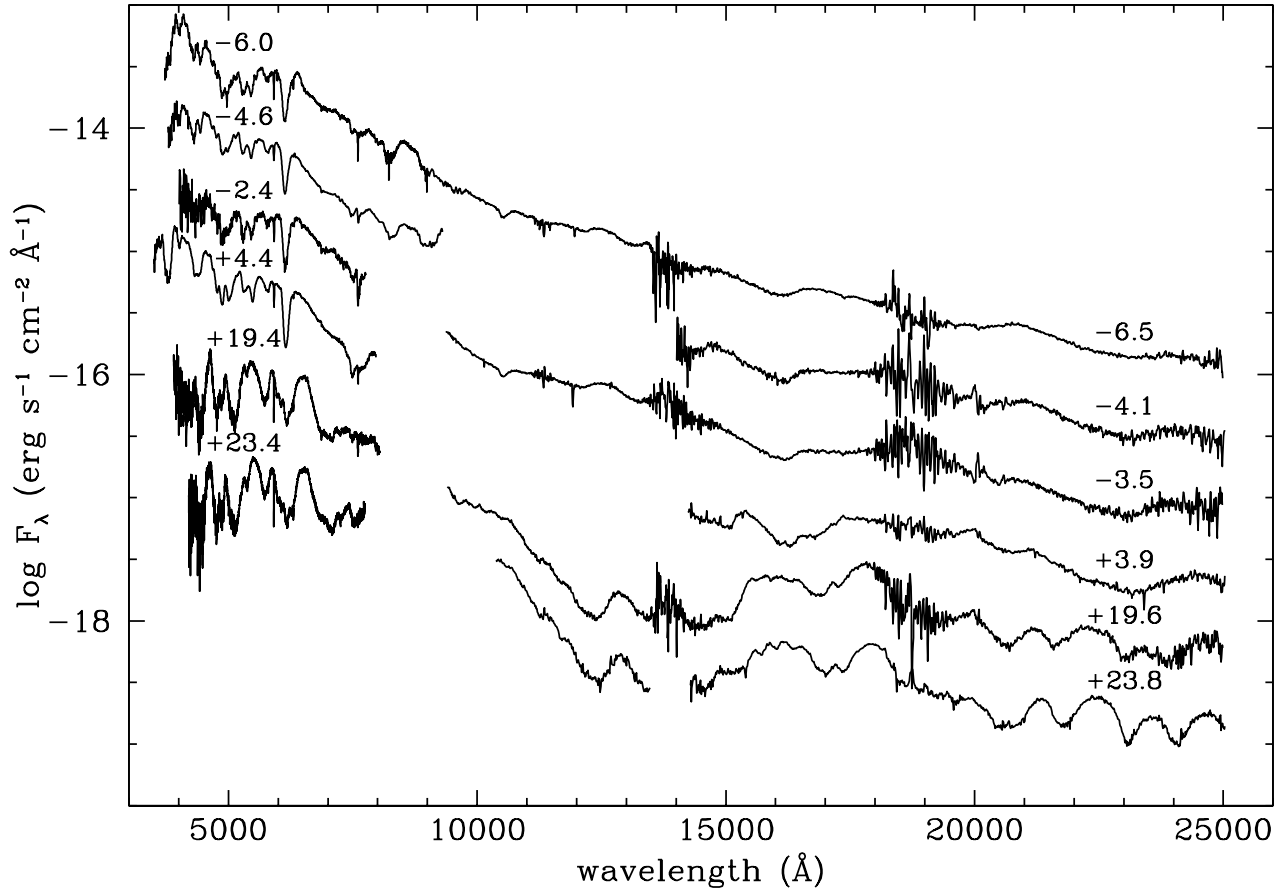


Figure 15. Combined optical and IR spectra, showing the evolution of SN 2003cg from 1 week before to 3 weeks after maximum light. The spectra have been corrected for reddening due to the Milky Way and the host galaxy.

5.4.1 Days $-7.6/-6.5$

Here we model the day -7.6 spectrum optical spectrum and day -6.5 NIR spectrum, which were among the earliest obtained. In the model, the SN ejecta above the photosphere is divided into three spherically symmetric shells above 11200, 11600, and 15500 km s^{-1} , respectively. All shells are dominated by O (48% to 64% by mass). The outermost shell contains 5% C to account for the C II line (see below). A rather high amount of Si (18% to 25% in the inner shell) is necessary to reproduce the deep Si II features in the spectrum. Also of interest is the high Fe group abundance at this early stage. We find 5% Ni in all shells. The stable Fe abundance, i.e. Fe that is not produced in the Ni decay chain, is between 1.5% near the photosphere, and 0.5% in the outermost shell. Finally, Ti and Cr of $\approx 0.5\%$ are needed in order to shift the flux from the UV to optical wavelengths. The best fit was achieved using $\log_{10} L = 42.88$ (erg s^{-1}), a photospheric velocity $v_{ph} = 10,300$ km s^{-1} , and epoch after explosion $t_{exp} = 12.3$ d (i.e. a rise time of 19.9 days, cf. Section 4.1.1). The observed spectrum, dereddened according to the prescription derived above (Section 3), and the synthetic spectrum are compared in Figure 20 (top), where the main features are also identified.

The model reproduces the overall shape and the individual line profiles reasonably well, but it has difficulties matching the very blue $B - V$ colour obtained through the dereddening procedure adopted. In particular, in order to obtain a blue continuum we have to adopt a rather low value for the photospheric velocity. This leads to near-photospheric temperatures that are too high, and results in the presence of lines in the synthetic spectrum that are not present in the observed one. In particular this affects Si III lines.

Starting at the blue end of the spectrum, the strong Ca II H&K near 3800 Å can be seen. The narrow feature at ≈ 4000 Å is identified as Si II 4130 Å. The peak near 4000 Å is suppressed in the model due to Si III absorptions. This indicates that the temperature near the photosphere is too high. The excessive strength of two other Si III lines, 4565 Å, which is seen in the model near 4400 Å, and 5740 Å, seen near 5500 Å, substantiates this assumption. The absorption at 4250 Å is a combination of Mg II 4481 Å, Fe III 4420 Å, and Si III 4339 Å. The feature slightly blueward of 5000 Å is caused by Si II 5056 Å and Fe III 5128, 5156 Å. In this case the presence of strong Fe III lines is supported by the accuracy with which the observed profile is matched. Near 5300 Å, we recognize the typical Si II W-feature, followed by the two Si II

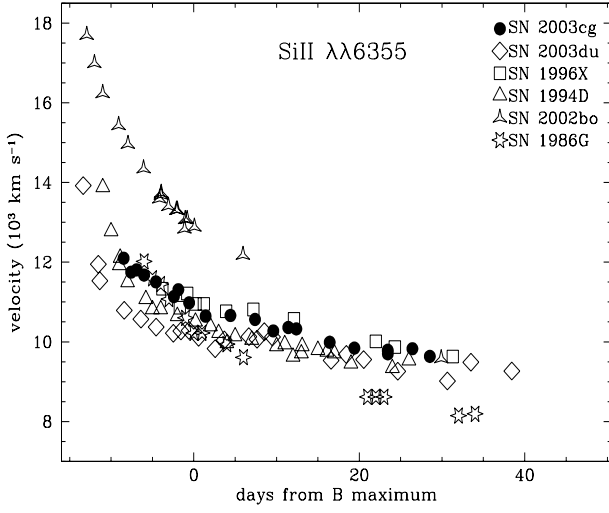


Figure 16. Evolution of the expansion velocity derived from the minima of Si II 6355 Å for SN 2003cg, compared with other LVG SNe: SN 2003du (Stanishev et al., 2004, in preparation), SN 1996X (Salvo et al. 2001) and SN 1994D (Patat et al. 1996). Also shown are the evolution of the HVG SN 2002bo (Benetti et al. 2004) and the FAINT SN 1986G (Cristiani et al. 1992, Benetti et al. 2005).

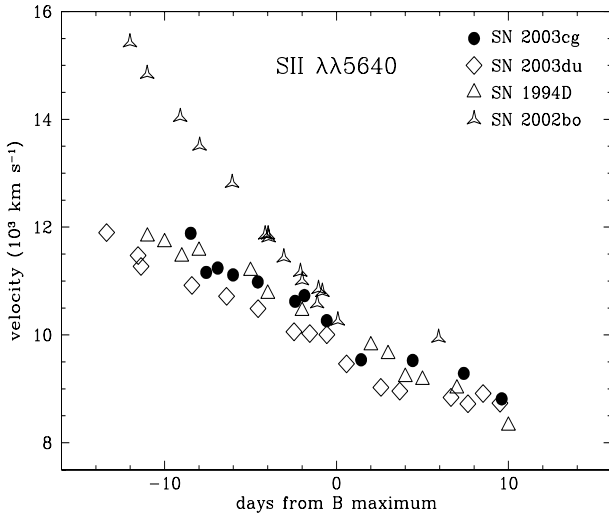


Figure 17. Evolution of the expansion velocity derived from the minima of Si II 5640 Å for SN 2003cg, and two other LVG SNe: SN 2003du, SN 1994D. Also shown is the evolution of the HVG SN 2002bo.

lines at 5960Å and 6350Å. The weakness of the synthetic Si II 5960Å line again suggests that the model temperature near the photosphere is too high. The emission component of the Si II 6350Å line is suppressed in the observed spectrum. This effect is reproduced in the model by C II 6580Å absorption. This has also been detected in other SNe Ia (e.g. Mazzali 2001). Further to the red only two more lines are clearly identified: O I 7774Å, and the Ca II IR triplet. Both

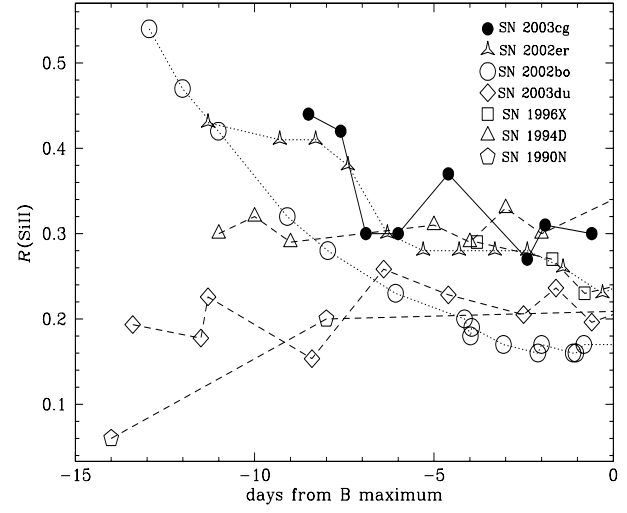


Figure 18. Pre-maximum evolution of $\mathcal{R}(\text{Si II})$ for SN 2003cg, compared with those SNe 2002er, 2002bo (HVG) 2003du, 1996X, 1994D and 1990N (LVG) (Benetti et al. 2005).

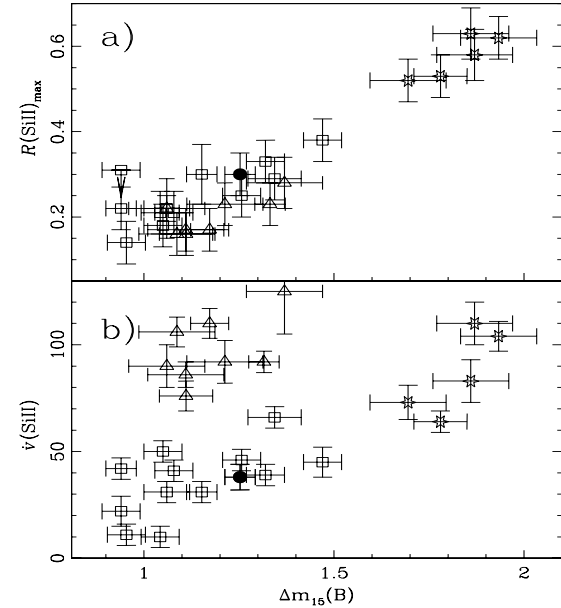


Figure 19. a) $\mathcal{R}(\text{Si II})_{\max}$ vs. $\Delta m_{15}(\text{B})$. b) \dot{v} vs. $\Delta m_{15}(\text{B})$ for Si II 6355. Filled symbols refer to SN 2003cg, and squares, triangles and stars represent LVG, HVG and FAINT SNe, respectively (Benetti et al. 2005).

lines are somewhat deeper in the model. An absorption in the synthetic spectrum near 9000Å is attributed to a blend of Mg II 9218Å, Si III 9324Å, and Si II 9413Å.

In Figure 20 (bottom) we compare the day -6.5 NIR spectrum with the model spectrum described above, extended to the NIR. Owing to the black body lower boundary adopted in the model, the predicted IR continuum exceeds

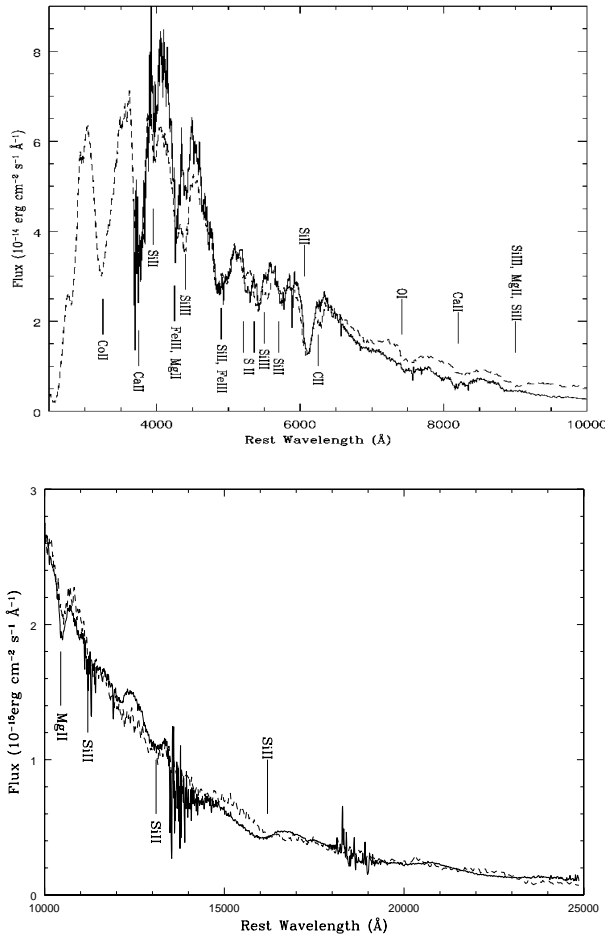


Figure 20. Observed, dereddened optical (top) and NIR (bottom) spectra of SN 2003cg at day $-7.6/-6.5$ and corresponding spectral models. The models parameters include $\log_{10} L = 42.88$ (erg s^{-1}), $v_{ph} = 10,300 \text{ km s}^{-1}$, $\mu = 31.28$ and $t_{exp} = 12.3 \text{ d}$.

that observed. We attribute this to a drop in opacity which appears redward of $\sim 7000 \text{ \AA}$ and is not reproduced in the model (see Figure 20 - top). Therefore, to match the observed spectrum, the model continuum was multiplied by a factor 0.5. However, apart from the discrepancy in the overall flux level, the shape of the IR continuum and other features are well reproduced by the model at this epoch. Only a few, relatively weak lines are present in the NIR spectrum, primarily due to Si II and Mg II. The feature at 1.05μ is well reproduced by Mg II 10914, 10951 \AA . As well discuss Hatano et al. (1999) in their work (see also Section 5.2), the identification of Mg II at this wavelength implies the presence of other Mg II features in other parts of the optical/NIR spectrum, some of which have been identified above. In spite of this and due the lower stretch of this lines in the observed spectra, we can not exclude the presence of He 10830 \AA .

5.4.2 Day -0.6

We have also modelled the SN 2003cg optical spectrum near maximum light. The dereddened day -0.6 spectrum

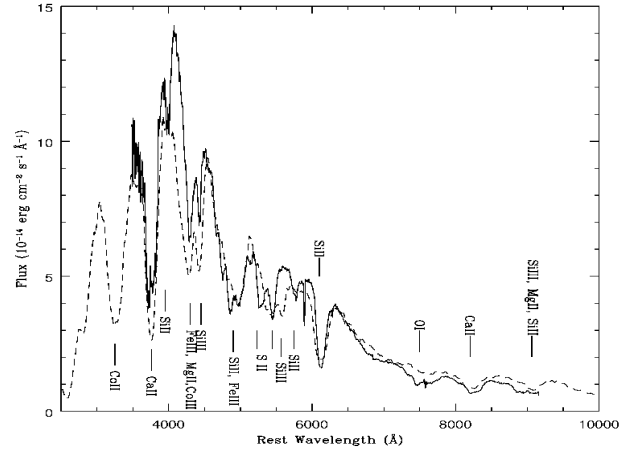


Figure 21. Observed, dereddened optical spectrum of SN 2003cg at day -0.6 and corresponding spectral model. The model parameters include $\log_{10} L = 43.11$ (erg s^{-1}), $v_{ph} = 6,000 \text{ km s}^{-1}$, $\mu = 31.28$ and $t_{exp} = 19.3 \text{ d}$.

was compared to a synthetic spectrum computed using the following parameters: $t_{exp} = 19.3 \text{ d}$, $\log_{10} L = 43.11$ (erg s^{-1}) and $v_{ph} = 6000 \text{ km s}^{-1}$. The observed spectrum, dereddened as above, and the synthetic spectrum are compared in Figure 21, where the main features are also identified.

As for the pre-maximum spectrum, we are forced to use a very low velocity for this epoch because the dereddened spectrum is unusually blue. Our synthetic spectrum has $B - V \sim 0.0$, but the dereddened spectrum has $B - V \sim -0.2$. Therefore, on the one hand our model colour is too red, and on the other our model line features are somewhat too hot compared to the observed ones.

The features present in the spectrum are generally similar to those deduced in the -7.6 day spectrum. In the blue region Ca II H&K is strong. Si II 4130 \AA is present in the data but not reproduced in the model. The line near 4300 \AA is now dominated by Fe III 4419, 4431 \AA , and Co III 4433 \AA , while Mg II 4481 \AA makes only a minor contribution. Moving redwards, we again identify Si III 4560 \AA . This line is strong both in the observed spectrum and in the synthetic one. However, other lines of Si III, notably 5740 \AA , which is strong in the model near 5500 \AA , but are absent in the data, indicate that the model temperature is too high. The feature near 5000 \AA is dominated by Fe III 5127, 5156 \AA , with contributions from Si II 5056 \AA and Fe II 5169 \AA . The observed profile of this feature however suggests that Fe II lines also make an important contribution. The Si II W-feature is affected by the presence of Si III 5740 \AA . The prominent Si II 6350 \AA line is well reproduced with an increased Si abundance (reaching $\sim 40\%$ near the photosphere). The Si II 5960 \AA is however not reproduced at all, again indicating that the adopted velocity and luminosity lead to a temperature that is too high. By this epoch, the C II line on top of the Si II 6350 \AA emission has vanished. This is because the density in the outermost layers, where carbon is found, is now too low for the line to form. Further to the red we identify strong O I 7774 \AA , and the Ca II IR triplet. Finally, we identify another strong absorption at 9000 \AA due mostly to Si III 9324 \AA .

6 SUMMARY

SN 2003cg is a heavily reddened but otherwise normal Type Ia supernova. We have presented the results of an intensive optical/NIR monitoring programme by the ESC using a wide range of telescopes and instruments. Photometry and spectroscopy were acquired spanning day -8 to +414 after B maximum light (plus upper limits on day +624). We have corrected all our photometric measurements for the deviation of each instrumental photometric setup from the Bessell (optical) and Persson (IR) standard systems. This was done using the S-correction method, and was applied up to the latest observed phases.

Besides the atypically red observed colours, evidence for high extinction towards SN 2003cg include (a) its coincidence with a dust lane of NGC 3169, (b) the very strong NaID interstellar doublet and (c) the presence of a *diffuse interstellar band* (DIB). However, dereddening using a standard extinction law to match a typical SN Ia $B - V$ colour yields a peak absolute magnitude at maximum which is abnormally bright. We therefore allowed R_V to become a free parameter within the CCM extinction law and adjusted R_V and $E(B - V)$ to provide simultaneous matches to a range of colour curves of normal SNe Ia. From this, we obtained $E(B - V) = 1.33 \pm 0.11$ and $R_V = 1.80 \pm 0.20$. While the value obtained for R_V is small, such values have been invoked in the past. It implies that the grain size is small compared with the average value for the local ISM. As an alternative explanation, the light echo (LE) hypothesis (Wang 2005), has severe difficulties. It seems unlikely that dust as close as $R_0 \leq 10^{16}$ cm could survive the supernova peak luminosity. If a significant proportion did survive it would produce a strong NIR excess, but this is not seen. Other LE effects expected but not seen in SN 2003cg, include (a) a reduced $(B - V)$ color range, (b) temporal variation in the reddening, (c) an anomalously small Δm_{15} , (d) a significantly brighter late phase tail and (e) broader spectral lines (more details in Patat et al. 2005).

The shape of the UBVR_IHK light curves of SN 2003cg are generally typical of a normal Type Ia SN. The U and V light curves show a broader peak and a pronounced shoulder in the post-maximum decay, respectively. Again we believe that this is due to the high reddening, causing the effective λ of these bandpasses to shift to redder wavelengths. We obtain a reddening-corrected $\Delta m_{15}(B)_{obs} = 1.25 \pm 0.05$ for SN 2003cg, which is typical for normal SNe Ia. The intrinsic peak bolometric luminosity is $\log_{10} L = 43.01 \pm 0.05$ (erg s⁻¹).

The spectral evolution of SN 2003cg is also similar to that of other normal Type Ia SN. This includes the spectral features, their ratios and their evolution. The earliest spectra exhibit a weak, but clearly visible, high velocity component of Ca II IR. The late phase spectra show emission features of [Fe II], [Fe III] and [Co II] plus an unusual blend of lines between 7100 and 7350 Å. From the velocity evolution of Si II at 6355 Å and S II at 5640 Å, we classify SN 2003cg as an LVG SN. The same conclusion is indicated by the $\mathcal{R}(\text{SiII})$ evolution.

SN 2003cg, the fourth target followed by the ESC,

has provided an important addition to the database of well-monitored nearby Type Ia. In addition, further study of the heavy reddening towards SN 2003cg will help us to establish the diversity in the characteristics of dust responsible for astrophysical extinction.

ACKNOWLEDGMENTS

We are grateful to the Visiting Astronomers of all telescopes who kindly observed SN 2003cg as a *Target of Opportunity*. We thank also J. Méndez's help in acquiring the TNG+OIG observations, V. Stanishev for providing us their data of SN 2003du prior to publication and J. A. Caballero for providing us a macro for NIR data reduction. This work is supported in part by the European Community's Human Potential Programme under contract HPRN-CT-2002-00303, "The Physics of Type Ia Supernovae". This work is based on observations collected at the European Southern Observatory, Chile under programmes ID 071.A-9006(A), ID 071.D-0281(D), ID 073.D-0853(A,B,C,D), 074.D-0340(E), at the Calar Alto Observatory (Spain), the Italian Telescopio Nazionale Galileo (La Palma), the Isaac Newton and William Herschel Telescopes of the Isaac Newton Group (La Palma), the Asiago Observatory (Italy), the Beijing Observatory (China), the Siding Spring Observatory (Australia) and the United Kingdom Infrared Telescope (Hawaii). The TNG is operated on the island of La Palma by the Centro Galileo Galilei of INAF (Istituto Nazionale di Astrofisica) at the Spanish Observatorio del Roque de los Muchachos of the Instituto de Astrofísica de Canarias. The INT, JKT and WHT are operated on the island of La Palma by the Isaac Newton Group (ING) in the Spanish Observatorio del Roque de los Muchachos of the Instituto de Astrofísica de Canarias. UKIRT is operated by the Joint Astronomy Centre on behalf of the U.K. Particle Physics and Astronomy Research Council. Some of the data reported here were obtained as part of the ING and UKIRT Service Programmes. This work has made use of the NASA/IPAC Extragalactic Database (NED) which is operated by the Jet Propulsion Laboratory, California Institute of Technology, under contract with the National Aeronautics and Space Administration.

REFERENCES

- Alard C., 2000, A&AS, 144, 363
- Altavilla G. et al., 2004, MNRAS, 349, 1344
- Axelrod T.S., PhD thesis, Univ. California at Santa Cruz
- Barbon R. et al., 1990, A&A, 237, 79
- Benetti S., 2000, MmSAI, 71, 323
- Benetti S. et al., 2004, MNRAS, 348, 261
- Benetti S. et al., 2005, ApJ, 623, 1011
- Benetti S., 2005, in Turatto M., Benetti S., Zampieri L. & W. Shea, eds., Supernovae as Cosmological Lighthouse. Astron. Soc. Pac., San Francisco, p. 235
- Bessell M. S., 1990, PASP, 102, 1181
- Branch D. & Tammann G. A., 1992, ARA&A, 30, 359
- Bowers E. J. C. et al., 1997, MNRAS, 290, 663
- Calzetti D., 2001, PASP, 113, 1449
- Capaccioli M. et al., 1990, ApJ, 350, 110
- Cardelli J. A., Clayton G. C. & Mathis J. S., 1989, ApJ, 345, 245

- Chini R. & Wargau W. F., 1990, *A&A*, 227, 213
- Contardo G., Leibundgut B. & Vacca W. D., 2000, *A&A*, 359, 876
- Clayton G. C., 2004, in Witt A. N., Clayton G. C. & Draine B. T., eds., *ASP Conf. Ser. Vol. 309, Astrophysics of Dust*. Astron. Soc. Pac., San Francisco, p. 57
- Cristiani S. et al., 1992, *A&A*, 259, 63
- Dopita M. A. et al., 1984, *ApJ*, 287, L69
- Dwek E., 1983, *ApJ*, 274, 175
- Fitzpatrick E. L., 1999, *PASP*, 111, 63
- Fitzpatrick E. L., 2004, in Witt A. N., Clayton G. C. & Draine B. T., eds., *ASP Conf. Ser. Vol. 309, Astrophysics of Dust*. Astron. Soc. Pac., San Francisco, p. 57
- Freedman W. L. et al., 2001, *ApJ*, 553, 47
- Gaskell C. M., 1984, *PASP*, 96, 789
- Gaskell C. M. & Keel W. C., 1986, *BAAS*, 18, 953
- Geminale A. & Podowski P., 2005, preprint (astro-ph/0502540)
- Geminale A., 2006, PhD thesis, Univ. Padova (Italy).
- Gibson B. K. et al., 2000, *ApJ*, 529, 723
- Goldhaber G. et al., 2001, *ApJ*, 558, 359
- Hamuy M. et al., 1992, *PASP*, 104, 533
- Hamuy M. et al., 1994, *PASP*, 106, 566
- Hamuy M. et al., 1996, *AJ*, 112, 2391
- Hamuy M. et al., 2002, *AJ*, 124, 417
- Hamuy M. et al., 2003, *Nature*, 424, 651
- Hatano K. et al., 1999, *ApJ*, 525, 881
- Henry R. B. C. & Branch D., 1987, *PASP*, 99, 112
- Herbig G. H., 1995, *ARA&A*, 33, 19
- Höflich P. et al., 2004, *ApJ*, 617, 1258
- Itagati K. & Arbour R., 2003, *IAUC* 8097
- Jansen R. A. et al., 1994, *MNRAS*, 270, 373
- Jha S., 2002, PhD thesis, Harvard University
- Knop R. A. et al., 2003, *ApJ*, 598, 102
- Kotak R., Meikle W. P. S. & Patat F., 2003, *IAUC* 8099
- Kotak R. et al., 2004, *MNRAS*, 354, L13
- Kotak R. et al., 2005, *A&A*, 436, 1021
- Kraan-Korteweg R. C., 1986, *A&AS*, 66, 255
- Krisciunas K. et al., 2000, *ApJ*, 539, 658
- Krisciunas K. et al., 2003, *AJ*, 125, 166
- Krisciunas K. et al., 2004a, *AJ*, 127, 1664
- Krisciunas K. et al., 2004b, *AJ*, 128, 3034
- Krisciunas K. et al., 2005, *AJ* in press (astro-ph/0511162)
- Landolt A.U., 1992, *AJ*, 104, 340
- Lira P., 1995, M. S. thesis, University of Chile
- Lucy L.B., 1999, *A&A*, 345, 211
- Matheson T. et al., 2003, *IAUC* 8099
- Mazzali P. A. & Lucy L. B., 1993, *A&A*, 279, 447
- Mazzali P. A. & Lucy L. B., 1998, *MNRAS*, 295, 428
- Mazzali P. A. et al., 1998, *ApJ*, 499, L49
- Mazzali P. A., 2000, *A&A*, 363, 705
- Mazzali P. A., 2001, *MNRAS*, 321, 341
- Mazzali P. A. et al., 2005, *ApJ*, 623, L37
- Meikle W. P. S. et al., 1996, *MNRAS*, 281, 263
- Meikle W. P. S., 2000, *MNRAS*, 314, 782
- Meikle W. P. S., Khreegi Y. & Kotak R., 2005, in Turatto M., Benetti S., Zampieri L. & W. Shea, eds., *Supernovae as Cosmological Lighthouse*. Astron. Soc. Pac., San Francisco, p. 217
- Metlova N. V., 1985, *IBVS*, 2780, 1M
- Munari U. & Zwitter T., 1997, *A&A*, 318, 269
- Nomoto K., Thielemann F. K. & Tokoi K., 1984, *ApJ*, 286, 644
- Nomoto K. et al., 2003, in Leibundgut B., Hillebrandt W., eds, *Proc. to the ESO/MPA/MPE Workshop (an ESO Astrophysics Symp.) From Twilight to Highlight the Physics of Supernovae*. Springer-Verlag, Berlin, p.115
- Nugent P. et al., 1995, *ApJ*, 455, L147
- Nugent P., Kim A. & Perlmutter S., 2002, *PASP*, 114, 803
- O'Donnell J. E., 1994, *ApJ*, 422, 158
- Patat F. et al., 1996, *MNRAS*, 278, 111
- Patat F. et al., 2005, preprint (astro-ph/0512574)
- Pauldrach, A.W.A. et al., 1996, *A&A* 312, 525
- Perlmutter S. et al., 1997, *ApJ*, 483, 565
- Perlmutter S. et al., 1999, *ApJ*, 517, 565
- Persson S. E. et al., 1998, *AJ*, 116, 2475
- Phillips M. M., 1993, *ApJ*, 413, L105
- Phillips M. M. et al., 1999, *AJ*, 118, 1766
- Pignata G. et al., 2004a, *MNRAS*, 355, 178
- Pignata G., 2004b, PhD thesis, Univ. Padova (Italy).
- Pozzo M. et al., 2006, *MNRAS* in press (astro-ph/0602372).
- Reindl B. et al., 2005, *ApJ*, 624, 532
- Riess A. G. et al., 1998, *AJ*, 116, 1009
- Riess A. G. et al., 1999, *AJ*, 118, 2688
- Salvo M. E. et al., 2001, *MNRAS*, 321, 254
- Savage B. D. & Mathis J. S., 1979, *Ann. Rev. Astr. Ap.*, 17, 73
- Schaefer B., 1995, *ApJ*, 450, L5
- Schlegel D. J., Finkbeiner D. P. & Davis M., 1998, *ApJ*, 500, 525
- Seaton M. J., 1979, *MNRAS*, 187, 73p
- Spyromilio J. et al., 1992, *MNRAS*, 258, 53P
- Stritzinger M. et al., 2002, *AJ*, 124, 2100
- Stehle M. et al., 2005, *MNRAS*, 360, 1231
- Suntzeff N. B., 1996, in McCray R., Wang Z., eds, *Proc. IAU Colloquium 145, Supernovae and Supernova Remnants*, Cambridge: University Press, p. 41
- Suntzeff N. B., 2000, *American Institute of Physics Conference Series*, 522, 65
- Suntzeff N. B., 2003, in Leibundgut B., Hillebrandt W., eds, *Proc. to the ESO/MPA/MPE Workshop (an ESO Astrophysics Symp.) From Twilight to Highlight the Physics of Supernovae*. Springer-Verlag, Berlin, p.183
- Turatto M. et al., 1990, *AJ*, 100, 771
- Turatto M., Benetti S. & Cappellaro E., 2003, in *From Twilight to Highlight the Physics of Supernovae*, Leibundgut B., Hillebrandt W., eds., Springer-Verlag, Berlin, p. 200
- Wang L., 2005, *ApJ*, 635, L33
- Wang X. et al., 2005, *ApJ*, 620, L87
- Wheeler J. C. et al., 1998, *ApJ*, 496, 908

Table 11. Main data of SN 2003cg and its host galaxy.

Host Galaxy Data	NGC 3169	Ref.
α (2000)	$10^h 14^m 15^s 00$	1
δ (2000)	$03^\circ 27' 58''$	1
Galaxy type	SA(s)a pec	1
B magnitude	11.08	1
Galactic extinction A_B	0.134	2
v_r (km s $^{-1}$)	1238	1
μ	31.28	3
SN Data	SN 2003cg	Ref.
α (2000)	$10^h 14^m 15^s 97$	4
δ (2000)	$03^\circ 28' 02'' 50$	4
Offset SN-Gal. nucleus	$14'' E, 5'' N$	4
Discovery date (UT)	2003 March 21.51	4
Discovery date (MJD)	52719.51	4
E(B–V)	1.33 ± 0.11	5
R_V	1.80 ± 0.19	5
Date of B max (MJD)	52729.40 ± 0.07	5
Magnitude and epoch at max respect B max	U = 16.64 ± 0.03 ; -1.6 (days) B = 15.94 ± 0.04 ; 0.0 (days) V = 14.72 ± 0.04 ; +0.8 (days) R = 14.13 ± 0.05 ; +0.5 (days) I = 13.82 ± 0.04 ; -1.7 (days) J = 13.55 ± 0.05 ; -2.6 (days) H = 13.69 ± 0.05 ; -0.2 (days) K = 13.40 ± 0.02 ; -0.7 (days)	5 5 5 5 5 5 5 5
Magnitude and epoch of second IJHK max respect B max	I = 14.19 ± 0.02 ; +26.4 (days) J = 14.50 ± 0.06 ; +31.4 (days) H = 13.74 ± 0.02 ; +23.1 (days) K = 13.52 ± 0.02 ; +22.3 (days)	5 5 5 5
$\Delta m_{15}(B)_{obs}$	1.12 ± 0.04	5
$\Delta m_{15}(B)_{intrinsic}$	1.25 ± 0.05	5
$t_r(B)$	19.9 ± 0.5	5
stretch factor in B	0.97 ± 0.02	5
ΔC_{12}	0.39 ± 0.11	5
Absolute magnitude	$M_U^{max} = -19.63 \pm 0.94$ $M_B^{max} = -19.26 \pm 0.75$ $M_V^{max} = -19.06 \pm 0.49$ $M_R^{max} = -18.83 \pm 0.35$ $M_I^{max} = -18.32 \pm 0.19$ $M_J^{max} = -18.23 \pm 0.14$ $M_H^{max} = -17.92 \pm 0.11$ $M_K^{max} = -17.97 \pm 0.06$	5 5 5 5 5 5 5 5
$\log_{10} L$	43.01 ± 0.05 (erg s $^{-1}$)	5
E(U-B)	1.08 ± 0.13	5
E(V-R)	0.64 ± 0.06	5
E(R-I)	0.74 ± 0.11	5
E(V-J)	2.03 ± 0.20	5
E(V-H)	2.34 ± 0.09	5
E(V-K)	2.45 ± 0.23	5

(1) NED; (2) Schlegel, Finkbeiner & Davis (1998); (3) Assuming a Virgo distance of 15.3 Mpc (Freedman et al. 2001) and a relative distance from Virgo of 1.18 for NGC 3169 (Kraan-Korteweg 1986); (4) Itagati & Arbour (2003); (5) This work.